2019-08-28

Notch Coordinates Periodontal Ligament Maturation through Regulating Lamin A

Denes, BJ

10.1177/0022034519871448
Journal of Dental Research
SAGE Publications

Journal of
Dental Research

Notch coordinates periodontal ligament maturation through regulating Lamin A

Journal:	*Journal of Dental Research*
Manuscript ID	JDR-19-0375.R2
Manuscript Type:	Research Reports
Date Submitted by the Author:	31-Jul-2019
Complete List of Authors:	Denes, Balazs; Universite de Geneve, Orthodontics Bolton, Chloe; Peninsula Dental School Illsley, Charlotte; Peninsula Dental School Kok, Wai Ling; Peninsula Dental School Walker, Jemma; Plymouth University Peninsula Schools of Medicine & Dentistry, Peninsula Dental School Poetsch, Ansgar ; University of Plymouth, School of Biomedicine, Faculty of Medicine and Dentistry Tredwin, Christopher; Peninsula Dental School Kiliaridis, Stavros; Univ. Geneve, , Dept Orthodontics Hu, Bing; Peninsula Dental School,
Keywords:	Tooth development, Periodontal ligament (PDL), Occlusion, Molecular biology, Cell biology
Abstract:	Tooth eruption is a continuous biological process with dynamic changes at cellular and tissue levels particularly within the periodontal ligament (PDL). Occlusion completion is a significant physiological landmark of dentition establishment. However the importance of the involvement of molecular networks engaging in occlusion establishment on the final PDL maturation are still largely unknown. In this study, using rat and mouse molar teeth and a human PDL cell line for RNAseq and proteomic analysis, we systematically screened the key molecular links in regulating PDL maturation before and after occlusion establishment. We discovered Notch, a key molecular pathway in regulating stem cell fate and differentiation, is a major player in the event. Intercepting Notch pathway by deleting its key canonical transcriptional factor: RBP-Jkappa using conditional knock out strategy in the mice delayed PDL maturation. We also identified that Lamin A, a cell nuclear lamina member, is one unique marker of PDL maturation and its expression is under the control of Notch signalling. Our study therefore provides a deep insight of how PDL maturation is regulated at molecular level and we expect the outcomes to be applied for a better understanding of the molecular regulation networks in physiological conditions such as tooth eruption and movement, and also for periodontal diseases.

Date submitted: 4/19/2019
Date last revised: 7/31/2019
Date accepted: 8/2/2019

Notch coordinates periodontal ligament maturation through regulating Lamin A

Balazs Jozsef Denes[1], Chloe Bolton[2], Charlotte Sara Illsley[2], Wai Ling Kok[2], Jemma Victoria Walker[2], Ansgar Poetsch[3], Christopher Tredwin[2], Stavros Kiliaridis[1], Bing Hu[2*]

1. Department of Orthodontics, University Clinic of Dental Medicine, University of Geneva, Genève 4 CH, Rue Michel-Servet 1, 1211, Switzerland

2. Stem Cells & Regenerative Medicine Laboratory, Peninsula Dental School, Faculty of Medicine and Dentistry, University of Plymouth, 16 Research Way, Plymouth, PL6 8BU, United Kingdom

3. School of Biomedicine, Faculty of Medicine and Dentistry, University of Plymouth, 16 Research Way, Plymouth, PL6 8BU, United Kingdom

*Corresponding author

Prof. Bing Hu: bing.hu@plymouth.ac.uk

Running title: Notch controls periodontal ligament development

Key words: Tooth; Periodontal ligament; Occlusion; Notch, Lamin A

Abstract

Tooth eruption is a continuous biological process with dynamic changes at cellular and tissue levels particularly within the periodontal ligament (PDL). Occlusion completion is a significant physiological landmark of dentition establishment. However the importance of the involvement of molecular networks engaging in occlusion establishment on the final PDL maturation are still largely unknown. In this study, using rat and mouse molar teeth and a human PDL cell line for RNAseq and proteomic analysis, we systematically screened the key molecular links in regulating PDL maturation before and after occlusion establishment. We discovered *Notch*, a key molecular pathway in regulating stem cell fate and differentiation, is a major player in the event. Intercepting *Notch* pathway by deleting its key canonical transcriptional factor: *RBP-Jkappa* using conditional knock out strategy in the mice delayed PDL maturation. We also identified that *Lamin A*, a cell nuclear lamina member, is one unique marker of PDL maturation and its expression is under the control of *Notch* signalling. Our study therefore provides a deep insight of how PDL maturation is regulated at molecular level and we expect the outcomes to be applied for a better understanding of the molecular regulation networks in physiological conditions such as tooth eruption and movement, and also for periodontal diseases.

Introduction

Tooth eruption is accompanied by the development and maturation of PDL (Cho and Garant 2000). Recent studies suggest PDL originates from dental follicle progenitors that can be either *Osx Cre* (Ono et al. 2016) and/or *PTHrP-Cre* positive (Takahashi et al. 2019). During pre-occlusal eruption phase, a tooth performs axial movement till occlusion is reached, as such no exogenous tension or compression forces are applied on PDL yet. In parallel to the tooth eruption, mesenchymal cells inside PDL secrete increasing amounts of extracellular matrix such as collagen and elastin, which further polymerise into collagen fibres and elastic fibres (Berkovitz and Moxham 1990). Upon contacting the opposite tooth, i.e. the occlusion is established and root development is completed. The PDL fibres are then organized into thick bundles and suspend the tooth in the alveolar socket, hence are under the challenge of constant stretching force, facilitating the tooth to adapt to the biting force and prevent tissue damages (Beertsen et al. 1997).

The molecular networks and mechanisms linking occlusion establishement with PDL development has not been previously systemically screened yet. In many systems, *Notch* signalling plays a key role in controlling stem cell maintenance and differentiation (Cheung and Rando 2013). Notch proteins are transmembrane receptors that act through cell-to-cell and cell-to-matrix signalling (Giaimo and Borggrefe 2018). Binding of Notch receptor to ligand leads to the cleavage of the receptor's intramembrane sites and releasing of the intracellular domain (ICD), which translocates into nucleus and binds to the RBP-Jkappa transcription effector complex. Notch receptors are also sensitive to extracellular forces, and a small amount of force can reveal the S2 cleavage site for proteinases, which leads to release of the ICD domain and gene transcription (Kopan and Ilagan 2009). In the tooth, increasing evidence suggests that *Notch* is essential in the pulp and cervical loop stem cell maintenance and terminal odontoblast differentiation, as well as in tooth pulp wound healing ((Kurpinski et al. 2010;

Lovschall et al. 2007), and Walker et al., in press). However, although *Notch* pathway has been implicated in inducing osteogenic differentiation of cultured PDL cells (Li et al. 2014; Nakao et al. 2009; Osathanon et al. 2013), its function in periodontal ligament development and particularly maturation has not been elucidated.

In this study, we provide novel *in vivo* and *in vitro* evidence highlighting the important role of *Notch* pathway in periodontal ligament development and maturation with nuclear lamina protein *Lamin A* as a direct target.

Materials & Methods

Animals

The Wistar rat and tooth eruption stages were determined based on data of a previous study (Denes et al. 2018) and verified by micro-CT scans. The work was approvied by the ethics committee of animal research of the Canton of Geneva (n° GE/72/15). *RBP-Jκappa*$^{loxp/loxp}$ and *Col1α2-Cre* mice are as reported previously (Hu et al. 2010).

Laser capture microdissection

Mandibles were dissected and immediately frozen in PrestoChill (Milestone, Type 51420) at -40°C and stored at -80°C. Sections were performed with a cryostat and transferred to PET-membrane slides with the CryoJane Tape system (Leica Biosystems). Slides were dehydrated successively with 70%, 95%, 100% EtOH at -20°C. Microdissection of the periodontal ligament (PDL) was performed at the cervical 1/3 PDL region. For each developmental stage, 4 individual animals were used.

RNAseq statistical analysis

RNA extraction was performed according to RNeasy Micro Kit (Qiagen®). RNA quantity and quality was evaluated with Agilent 2100 Bioanalyzer (Agilent Technologies). RIN number

equal or greater to 7 was required for the sample for analysis. Total RNA was amplified and Next-Generation Sequencing with the Illumina HiSeq 4000 was performed with protocol Smarter + Nextera and the reference genome Rattus Norvegicus. Quality was assessed by FastQC v.0.11.5 and resulted in values between 32 and 40 (error: 1/1'000 to 1/10'000). The reads (length=100 bp) were mapped with the STAR v2.5.3a software to the reference genome and showed good alignment percentage (71.7% ±5.9). Biological quality control and summarization were done with the PicardTools v2.9.0 with percentage of mRNA bases as average 63%. The normalization and differential expression analysis was performed with the R/Bioconductor package edgeR v.3.16.5 and statistical significance was assessed with General Linear Model, negative binomial distribution and a quasi-likelihood *F*-test. Threshold for significance was set at p-value <5% and fold change (FC)>1.5. The RNAseq data can accessed through number: GSE129458 from https://www.ncbi.nlm.nih.gov/geo/. Enrichment analysis of RNAseq was performed with GO Ontology database and analyzed with PANTHER Overrepresentation Test. Fischer test was used with false discovery rate (FDR) correction applied. Biological processes, molecular functions and cell compartment analyses were classified based number of genes.

Rat paraffin sections

The cryoembedded mandibles were washed in distilled water to remove MCC, fixed in 4% paraformaldehyde (Merck), decalcified in Osteosoft (Sigma-Aldrich) or 14% EDTA (pH7.4) for a period of 6-weeks, embedded in paraffin. The paraffin blocks were cut into sections of 3µm thickness at the second root-pair of the first molar for rat samples and 10µm for mouse teeth.

Immunohistochemistry/Immunofluorescence

4-5 individual animals were used for each genotype at each defined stage. Osteosoft (Sigma-Aldrich) or 14% EDTA (pH7.4) decalcified samples were cut into 3µm thickness sections. The sections were deparafinized and antigen retrieval was done in citrate buffer (pH8.0) at 98°C for 20 min or a microwave at 750w for 1 minute, followed by blocking in PBS containing 5% donkey serum, 0.25% cold water fish gelatine and 0.25% bovine serum albumin for 1h at room temperature and incubated with rimary antibodies for overnight at 4°C, and secondary antibodies for 2h at room temperature. and counterstained with 4'-6-diamidino-2-phenylindole (DAPI). Imaging was performed with a Leica DMI6000 confocal microscope. For immunohistochemistry, Vectastain with DAB substrate were used. For details please see Appendix Table 3. Goldner staining was used for collagen staining.

Cell cultures and treatment

Human periodontal ligament fibroblasts (hPLF, ScienCell, Catalog #2630) were cultured in DMEM/F-12 with 20% FBS and 1% Antibiotic-Antimycotic. For Jagged1 treatment, after overnight seeding and cell confluency reached to 70%, Jagged1 was added to the medium to reach to a final concentration of 100ng/ml. Cultures were fixed after 24h of Jag1 treatment with 4% PFA at room temperature for 20 minutes and then washed 2x with PBS (10mM).

Stretching experiments were performed with the stretching device and silicone membranes (Strex USA, ST-140-04) (Appendix Figure 1 and 2). The membranes were coated with rat tail collagen type I (Life Technologies, A1048301) and HCl at 1:1 ratio overnight at 37°C. Cells were seeded as $2x10^5$ cells per membrane. Cells were stretched for 6h, 12h and 24h at 37°C alongside controls.

Quantitative real-time RT-PCR

Tirpilated samples were used for each gene analysis. Total RNAs was extracted using the penol-chloroform technique and reverse transcription of was achieved with High-Capacity cDNA synthesis kit (Thermo Fisher Scientific), as previously described (Singer et al. 2019). The PCR reaction was performed with SYBR Green I Master Mix (Roche) on a LightCycler 480 II Real-Time PCR system (Roche Molecular Diagnostics) for 45 cycles. *36 beta4* gene was used as housekeeping gene to normalize samples with the $2^{-\Delta\Delta Ct}$ method. All analyses were performed with three replicates as described previously (Hu et al. 2012). For the primers used in this study please see Appendix Table 3.

Nanoscale Liquid Chromatographic−Electrospray Ionization−Tandem Mass Spectrometry (nLC−ESI−MS/MS)

Duplicted samples were used for the analysis. In-gel tryptic digestion of proteins was carried out as described in (Costa et al. 2018). Peptides were separated on an HSS T3 column (waters) and injected into an Orbitrap Elite MS using a 90 min gradient from 2 to 30% acetonitrile, 0.1% formic acid. Full MS scans in the orbitrap and fragmentation of 20 most intense precursors in parallel was done. Protein identification and label-free quantification was done with MaxQuant (Cox et al. 2014) and further statistical analysis with Perseus (Tyanova et al. 2016). Differential expression of fold change > 2 was analyzed with Gene Ontology (GO) enrichment of biological processes powered by Panther Database (pantherdb.org) and clustering was performed with String Database v11.0 (string-db.org). For *in vivo* proteomic analysis, electrospray ionization Liquid-Chromatography-Mass Spectrometry/Mass Spectrometry (ESI-LC-MSMS) was performed on rat mandible periodontal ligament, dissected with laser capture microdissection

technique. The results can be access with number: PXD013379 from https://www.ebi.ac.uk/pride/archive/.

Western Blotting

Cells were washed with HBSS, collected at 10,000 rpm for 10 minutes at 4°C. The pellet was re-suspended in ice-cold radioimmunoprecipitation assay buffer (89901, Pierce) with protease & phosphatase inhibitor cocktail (78442, Pierce) and incubated on ice for 30 minutes then spun down at 10,000rpm for 10 minutes at 4°C. The supernatant was collected and quantified with BCA method (23225, Pierce). Protein were separated with 4-12% NuPAGE Novex Bis-Tris gel and transferred to polyvinylidene membrane, detected with iBind Flex Western device (SLF2000S, Invitrogen). Antibodies were diluted in iBindFlex solution (SLF2020, Invitrogen). Membranes were scanned with C-DiGit scanner (Li-COR, 3600-00). For antibodies see Appendix Table 3.

Results

PDL has distinct gene expression profile changes upon occlusion establishment

We selected postnatal day 18 (P18, pre-occlusion eruption) and 28 (P28, 1 week after occlusion establishment) of the Wistar rat's second root pair of the first lower molar as the studying models. The eruption stage was confirmed by daily *in vivo* micro-CT imaging based on our previous study (Denes et al. 2018). Histological analysis and micro-CT confirmed that the root development of P18 tooth was at the initial elongation stage, while at P28 the root development reached near completion (Figure 1A and Appendix Figure 1A). Trichrome staining showed P28 PDL was aboundant with collagen fibres, comparing to P18 (Figure 1B). As well, P28 PDL expressed significiantly higher level of Periostin (Figure 1C). To explore the transcriptome changes of PDL, we next performed RNAseq analysis on the PDL at indicated

stages (RNAseq accession number: GSE129458). Among a total of 12,742 detected genes, we identified 1,090 genes were upregulated and 1,035 were downregulated with more than 1.5 fold changes with p value < 5%, at P28 comparing to P18 (Appendix Table 1). Gene enrichment analysis suggested P28 has significantly increased cellular process and protein binding events comparing to P18 (Figure 1D). Heatmap of genes identified by Metacore pathway map analysis shows consistent expression throughout samples (Figure 1E). Using GO analysis to examine the biological processes and Metacore process networks, as expected, we have identified that "biomineral tissue development" and "muscle contraction" are among the most significantly changed biological processes (Figure 1F and Appendix Figure 1B).

Notch signalling is dynamically changed before and after occlusion is established

String analysis suggested *Notch* pathway acted as a center of the molecular networks (Figure 2A). Metacore pathway map analysis further confirmed *PI3K* and *Notch* signalings are the top two pathways affected (Figure 2B). As the function of *Notch* signaling has not been decribed previously in PDL *in vivo*, particularly in the occlusion establishing stage, we therefore continued focusing on that pathway for our study.

In the RNAseq analysis, *Notch1*, *Notch4* and *Dll1* are the *Notch* pathway members that were significantly upregulated in the P28 PDL comparing to P18 ($p<0.05$), and *Jagged 1* was upregulated with a marginal p value ($p = 0.067$), and *Furin* was significantly downregulated ($p<0.05$) (Figure 2C). We next compared Notch protein expression with immunofluorescence analysis. Consistent with the RNAseq results, we found that both total Notch1 and its ICD were increasingly expressed in the P28 PDL (Figure 2D and E) as well as Notch ligands such as Dll1 (Figure 2F), in parallel to the increased PDL maturation marker: Osteopontin (Figure 2G) (Rios et al. 2008). Interestingly, when we evaluated in parallel the other Notch receptor, Notch2 ICD's expression was at its highest level at pre-occlusal eruption stage and decreased thereafter

(Figure 2H), suggesting that Notch1 and Notch2 receptors play significant however different roles in PDL development.

Intercepting Notch pathway delays PDL development and tooth eruption

To confirm the function of *Notch* pathway in PDL development during occlusion establishment, we adopted the mesenchymal conditional *RBP-Jkappa* knockout transgenic mouse model, where the *Cre* recombinase expression is under the control of *Collagen 1 α2* promoter (Hu et al. 2010). Staining with specific antibodies, we observed abundant Cre protein expression in the PDL cells confirmed the deletion of the *RBP-Jkappa* gene in PDL cells, as well as osteoblasts at the bone surface (Figure 3A). By crossing the *Collagen 1 a2 Cre* transgenics with *RBP-Jkappa*$^{flox/flox}$ mice (Hu et al. 2012; Hu et al. 2010), phenotypically at P21 when the tooth eruption is complete in the WT mice, the mice with *RBP-Jkappa* deletion in PDL cells encountered significant delay of tooth eruption and root development (Figure 3B). Macroscopy analysis revealed the *RBP-Jkappa* knockout mice had smaller mandibles (Figure 3C) and molar crown size. (Figure 3D). Stereomicroscopy and microCT analysis and quantification (Figure 3G) suggested that while initially the root development is delayed in the *RBP-Jkappa* knockout mice (Figure 3E and G), the tooth crown eruption in the mutants could still be eventually completed (Figure 3F) and root length had no difference comparing the control with the knockout mice (Figure 3G). Consistantly, immunofluorescence analysis on Periostin expression suggested at P4 there were no expression of the marker (Appendix Figure 2A), while at P10 and P14 the knockout mice has a significantly delayed expression (Figure H&I). However, after two months there are no notable difference between the control and knockout animals' PDL (Figure 2J).

***In vitro* stretching mirrored occlusion establishment effects on PDL cells**

To confirm if the key molecular changes identified in the *in vivo* RNAseq analysis were due to the stretching of PDL mesenchymal cells and its relevance to human, we next cultured human PDL cells and mimicked occlusive stretching force by inducing reciprocal force on the cells on an automatic cell stretching system (Appendix Figure 2B and C). Real-Time RT-PCR results confirmed significant induction of the mRNA expression of *Notch* pathway members such as *Jagged 1*, *Dll1* and *Hey1* (Figure 4A), as well a panel PDL cell differentiation markers including Osteopontin (Figure 4B). To further gain insight of the molecular targets of the PDL in responding to stretching force, we performed proteomic analysis on the stretched PDL cells and found extracellular matrix protein such as collagen and periostin and the RhoA-CDC42 associated cytoskeleton regulating system were significantly changed (Figure 4C and D, and Appendix Table 2).

Lamin A is a direct effector in PDL in responding to stretching and act as Notch down-stream target

By comparing the *in vitro* PDL cell stretching results with proteomic analysis from the *in vivo* PDL maturation (PRIDE number: PXD013379) and RNAseq analysis, we noticed the nuclear membrane protein: Lamin A was the only molecule displaying the same upregulation pattern across the three analyses (Figure 5A). Immunofluorescent analysis confirmed that Lamin A/C expression did increase in the P28 rat PDL, comparing with P18 samples (Figure 5B). Western Blot analysis suggested Lamin A protein level is specifically induced in the stretched human PDL cells but not Lamin C (Figure 5C). Similarly, treating PDL cells with Notch ligand: Jagged1 could induce Lamin A expression (Figure 5D). Finally, in the *RBP-Jkappa* knockout mice PDL, Lamin A/C expression was concomitantly reduced both at P10 and 2 months (Figure 5E and F). Therefore, *Lamin A* is indeed an indicator of PDL maturation that is under *Notch* signalling control and is positively regulated by stretching force.

Discussion

The development of PDL, alveolar bone and cementum are closely linked events. So far, particularly for PDL and alveolar bone, it is still a dearth for finding genetic tools to dissect the specific populations inside the tissues, particularly for fibroblasts and osteoblasts. However, increasing evidence have already shown that multiple signalling pathways are closely involved in the periodontium development, such as *NFI-C* null mice abolish root development (Steele-Perkins et al. 2003) and conditional deletion of *Smad4* in tooth epithelium can impede root growth (Li et al. 2015), while conditional deletion PPR using PTHrP-Cre impede tooth eruption (Takahashi et al. 2019). *Notch* signalling is one of the key pathways in determining mesenchymal stem cell fate and cell differentiation such as in the muscles (Conboy et al. 2003; Conboy and Rando 2002). In bone and bone marrow mesenchymal progenitors, *Notch*'s function has been extensively descbed in protecting mesenchymal progenitors (Hilton et al. 2008). While in the tooth, previous reports and our findings suggest that *Notch* is important both for maintaining stem cells and differentiation but the functions are carried out via different Notch receptors: i.e. *Notch1* acts through maintaining stem cell pool and inducing cell differetnation and *Notch2* is rather responsible for maintaining transit amplying cells ((Mitsiadis et al. 2017; Zhang et al. 2008) and Walker et al. in press). In PDL, our results confirm that Notch1 is linked with PDL final development and completion, while interestingly Notch2 preferentially functions during the pre-occlusion stage. This might reflect a different role of *Notch2* in enhancing cell populating into the tissue, similar to the findings in the incisor mesenchymal stem cells (Walker et al. in press). Although we have not been able to achieve the mesenchymal specific conditional Notch receptor deletion models due to early death in embryonic stages (data not shown), it would be still interesting to apply inducible conditional deletion models to distinguish the different roles of Notch receptors in PDL development. As

well, future studying Notch's roles such as in PDL stem cell fate control, as well as aging are highly desired (Appendix Figure 3).

In addition, our results showed that blocking canonical *Notch* pathway by deleting *RBP-Jkappa* in the PDL delayed but did not inhibit tooth eruption and PDL maturation completely, suggesting that canonical *Notch* is dispensable in these events. Significantly, the Notch ligands: *Dll1*, *Dll4* and *Jagged1* expression are all highly elevated in the PDL cells upon stretching, suggesting the PDL cells play a central role in the tissue homeostasis, possibly through *Notch* pathway ligands production, to affect surrounding microenvironment, such as vascularisation through endothelial cell specific Notch4 receptor. One evidence to support this theory is that during orthodontic tooth movement, blood vessel proliferation and remodelling is among the early key events in the PDL (Rygh et al. 1986; Vandevska-Radunovic et al. 1994).

Lamin A is an important nuclear envelope molecule for protecting cells from DNA damage and pre-aging and its mutation can cause laminopathies including Progeria (Broers et al. 2006; Eriksson et al. 2003; Worman 2012). Lamin A gene encodes two isoforms: Lamin A and C that are created from alternative splicing that encode important protein for nuclear envelopes. While Lamin C is shorter and produced directly, Lamin A, which is two exons longer at C-terminal, is required to pass prelamin A stage followed by a series of posttranslational modifications initiated from the farneslation of C terminal cysteine (Lin and Worman 1993). We observed Lamin A transcription and translation were both elevated upon occlusion establishment, as well as under stretching condition in the PDL cells, which indicates its potential significant role in protecting the cells from stretching force induced cellular damages. The evidence that *Notch* signal activation by Jagged1 treatment could also elevate Lamin A but not Lamin C expression further confirmed that Lamin A potentially has significant role in PDL development and homeostasis, which requires additional investigations.

We hope our study is opening a new gateway and molecular clues for understanding how the PDL, one of the most dynamically changed tissues in the body, is maintained for homeostasis and integrity, not only in physiological conditions, but also for periodontal diseases.

Acknowledgement

We would like to thank the helps provided by platforms of the University of Geneva, including the iGE3 Genomics Platform, the Bioimaging Core Facility, the Histology Core Facility. This study was supported by the Swiss National Science Foundation grant n° FNRS 31003A_176131/1 to S. K., the European Union Marie Skłodowska-Curie Actions (618930, OralStem FP7-PEOPLE-2013-CIG), the European Regional Development Fund and the Biotechnology and Biological Sciences Research Council of the UK (BB/L02392X/1) to B.H. B.D., S.K. and B.H. contributed to conception and design of the work. B.D. and B.H. drafted the manuscript. B.D., C.B., C.I., W.K., J.W., A.P. and B.H. contributed to the acquisition and analysis of the data. C.T. and S.K. contributed to the interpretation of the data. All the authors critically revised the manuscript. The authors declare that there is no conflict of interest regarding the publication of this article.

Material and data availability statement

The materials used and datasets generated during and/or analysed during the current study are available from the corresponding author on reasonable request.

Reference

Beertsen W, McCulloch CA, Sodek J. 1997. The periodontal ligament: A unique, multifunctional connective tissue. Periodontol 2000. 13:20-40.

Berkovitz BK, Moxham BJ. 1990. The development of the periodontal ligament with special reference to collagen fibre ontogeny. J Biol Buccale. 18(3):227-236.

Broers JL, Ramaekers FC, Bonne G, Yaou RB, Hutchison CJ. 2006. Nuclear lamins: Laminopathies and their role in premature ageing. Physiol Rev. 86(3):967-1008.

Cheung TH, Rando TA. 2013. Molecular regulation of stem cell quiescence. Nat Rev Mol Cell Biol. 14(6):329-340.

Cho MI, Garant PR. 2000. Development and general structure of the periodontium. Periodontol 2000. 24:9-27.

Conboy IM, Conboy MJ, Smythe GM, Rando TA. 2003. Notch-mediated restoration of regenerative potential to aged muscle. Science. 302(5650):1575-1577.

Conboy IM, Rando TA. 2002. The regulation of notch signaling controls satellite cell activation and cell fate determination in postnatal myogenesis. Dev Cell. 3(3):397-409.

Costa MI, Cerletti M, Paggi RA, Trotschel C, De Castro RE, Poetsch A, Gimenez MI. 2018. Haloferax volcanii proteome response to deletion of a rhomboid protease gene. J Proteome Res. 17(3):961-977.

Cox J, Hein MY, Luber CA, Paron I, Nagaraj N, Mann M. 2014. Accurate proteome-wide label-free quantification by delayed normalization and maximal peptide ratio extraction, termed maxlfq. Mol Cell Proteomics. 13(9):2513-2526.

Denes BJ, Lagou A, Dorotheou D, Kiliaridis S. 2018. A longitudinal study on timing and velocity of rat molar eruption: Timing of rat molar eruption. Lab Anim. 52(4):394-401.

Eriksson M, Brown WT, Gordon LB, Glynn MW, Singer J, Scott L, Erdos MR, Robbins CM, Moses TY, Berglund P et al. 2003. Recurrent de novo point mutations in lamin a cause hutchinson-gilford progeria syndrome. Nature. 423(6937):293-298.

Giaimo BD, Borggrefe T. 2018. Introduction to molecular mechanisms in notch signal transduction and disease pathogenesis. Adv Exp Med Biol. 1066:3-30.

Hilton MJ, Tu X, Wu X, Bai S, Zhao H, Kobayashi T, Kronenberg HM, Teitelbaum SL, Ross FP, Kopan R et al. 2008. Notch signaling maintains bone marrow mesenchymal progenitors by suppressing osteoblast differentiation. Nat Med. 14(3):306-314.

Hu B, Castillo E, Harewood L, Ostano P, Reymond A, Dummer R, Raffoul W, Hoetzenecker W, Hofbauer GF, Dotto GP. 2012. Multifocal epithelial tumors and field cancerization from loss of mesenchymal csl signaling. Cell. 149(6):1207-1220.

Hu B, Lefort K, Qiu W, Nguyen BC, Rajaram RD, Castillo E, He F, Chen Y, Angel P, Brisken C et al. 2010. Control of hair follicle cell fate by underlying mesenchyme through a csl-wnt5a-foxn1 regulatory axis. Genes Dev. 24(14):1519-1532.

Kopan R, Ilagan MX. 2009. The canonical notch signaling pathway: Unfolding the activation mechanism. Cell. 137(2):216-233.

Kurpinski K, Lam H, Chu J, Wang A, Kim A, Tsay E, Agrawal S, Schaffer DV, Li S. 2010. Transforming growth factor-beta and notch signaling mediate stem cell differentiation into smooth muscle cells. Stem Cells. 28(4):734-742.

Li J, Feng J, Liu Y, Ho TV, Grimes W, Ho HA, Park S, Wang S, Chai Y. 2015. Bmp-shh signaling network controls epithelial stem cell fate via regulation of its niche in the developing tooth. Dev Cell. 33(2):125-135.

Li Y, Li SQ, Gao YM, Li J, Zhang B. 2014. Crucial role of notch signaling in osteogenic differentiation of periodontal ligament stem cells in osteoporotic rats. Cell Biol Int. 38(6):729-736.

Lin F, Worman HJ. 1993. Structural organization of the human gene encoding nuclear lamin A and nuclear lamin C. J Biol Chem. 268(22):16321-16326.

Lovschall H, Mitsiadis TA, Poulsen K, Jensen KH, Kjeldsen AL. 2007. Coexpression of notch3 and rgs5 in the pericyte-vascular smooth muscle cell axis in response to pulp injury. Int J Dev Biol. 51(8):715-721.

Mitsiadis TA, Caton J, Pagella P, Orsini G, Jimenez-Rojo L. 2017. Monitoring notch signaling-associated activation of stem cell niches within injured dental pulp. Front Physiol. 8:372.

Nakao A, Kajiya H, Fukushima H, Fukushima A, Anan H, Ozeki S, Okabe K. 2009. Pthrp induces notch signaling in periodontal ligament cells. J Dent Res. 88(6):551-556.

Ono W, Sakagami N, Nishimori S, Ono N, Kronenberg HM. 2016. Parathyroid hormone receptor signalling in osterix-expressing mesenchymal progenitors is essential for tooth root formation. Nat Commun. 7:11277.

Osathanon T, Manokawinchoke J, Nowwarote N, Aguilar P, Palaga T, Pavasant P. 2013. Notch signaling is involved in neurogenic commitment of human periodontal ligament-derived mesenchymal stem cells. Stem Cells Dev. 22(8):1220-1231.

Rios HF, Ma D, Xie Y, Giannobile WV, Bonewald LF, Conway SJ, Feng JQ. 2008. Periostin is essential for the integrity and function of the periodontal ligament during occlusal loading in mice. J Periodontol. 79(8):1480-1490.

Rygh P, Bowling K, Hovlandsdal L, Williams S. 1986. Activation of the vascular system: A main mediator of periodontal fiber remodeling in orthodontic tooth movement. Am J Orthod. 89(6):453-468.

Singer D, Thamm K, Zhuang H, Karbanova J, Gao Y, Walker JV, Jin H, Wu X, Coveney CR, Marangoni P et al. 2019. Prominin-1 controls stem cell activation by orchestrating ciliary dynamics. EMBO J. 38(2).

Steele-Perkins G, Butz KG, Lyons GE, Zeichner-David M, Kim HJ, Cho MI, Gronostajski RM. 2003. Essential role for nfi-c/ctf transcription-replication factor in tooth root development. Mol Cell Biol. 23(3):1075-1084.

Takahashi A, Nagata M, Gupta A, Matsushita Y, Yamaguchi T, Mizuhashi K, Maki K, Ruellas AC, Cevidanes LS, Kronenberg HM et al. 2019. Autocrine regulation of mesenchymal

progenitor cell fates orchestrates tooth eruption. Proc Natl Acad Sci U S A. 116(2):575-580.

Tyanova S, Temu T, Sinitcyn P, Carlson A, Hein MY, Geiger T, Mann M, Cox J. 2016. The perseus computational platform for comprehensive analysis of (prote)omics data. Nat Methods. 13(9):731-740.

Vandevska-Radunovic V, Kristiansen AB, Heyeraas KJ, Kvinnsland S. 1994. Changes in blood circulation in teeth and supporting tissues incident to experimental tooth movement. Eur J Orthod. 16(5):361-369.

Walker JV, Zhuang H, Singer D, Illsley CS, Kok WL, Sivaraj KK, Gao Y, Bolton C, Liu Y, Zhao M et al. 2019. Transit amplifying cells coordinate mouse incisor mesenchymal stem cell activation. Nature Communications. In press. **(Needs update prior to publication)

Worman HJ. 2012. Nuclear lamins and laminopathies. J Pathol. 226(2):316-325.

Zhang C, Chang J, Sonoyama W, Shi S, Wang CY. 2008. Inhibition of human dental pulp stem cell differentiation by notch signaling. J Dent Res. 87(3):250-255.

Figure legends

Figure 1. PDL express distinct molecular signatures upon occlusion establishment

A: Hematoxylin-Eosin (HE) staining of the P18 and P28 rat first lower molar.

B: Goldner staining of P18 and P28 PDL regions. Note the green-blue stained collagen fibers are abundant at P28 but not P18.

C: Immunofluorescent staining of Periostin with a specific antibody raised in rabbit then visualised using anti-Rabbit Alexa 568 (red) conjugated secondary antibody. Note the significantly increased Periostin signal at P28 comparing to P18.

D: Gene function enrichment analysis on the RNAseq results by comparing P28 with P18 PDL.

E, F: Differential analysis performed on the RNAseq results by comparing P28 with P18 PDL.

E: Metacore Pathway Maps heatmaps analysis.

D: GO analysis for the biological processes.

Bars: A: 100µm; B, C: 20µm.

Figure 2. Notch signalling has dynamic changes during PDL maturation

A: String analysis of the genes of top 10 pathways of the metacore Pathway Maps of the RNAseq results.

B: Metacore Pathway Maps analysis.

C: String analysis of the genes of top 10 pathways of the metacore Pathway Maps.

D: Notch pathway members that had significant changes in the RNAseq analysis.

D-H: Immunofluorescent analysis of the indicated molecules using specific primary antibodies. The Alexa 488 (green) or 568 (red) conjugated secondaries were used to identify the primary antibodies. Dotted lines mark the boundary between PDL and bone (B) or dentin (D).

Bars: 20μm

Figure 3. Intercepting canonical Notch pathway delayed PDL maturation

A: Immunostaining PDL of the second lower molars from P21 RBP-Jk $^{flox/flox}$ (control) and Collagen 1a2 Cre x RBP-Jk $^{flox/flox}$ (cKO) mice. Note the Cre positive signal could only be observed in the cKO mice.

B: HE staining of the P21 control and cKO mice second lower molars. Stars: PDL.

C, D: Stereo images of 1 month old control and cKO mouse mandibles and first lower molars. Note the cKO mouse tooth's crown size are smaller and roots are shorter than the control.

E: Representative stereo images of the first and third lower molars of the control and cKO mice at postnatal day 14.

F: Representative micro-CT analysis of the control and cKO fist lower molar eruption from 4 months old animals.

G: First lower molar mesial buccal root length comparisation at P14 and 2 months. ** $p<0.01$.

H-J: Immunofluorescent analysis of Periostin using specific primary followed by secondary antibodies (Alexa 568, red) at indicated stages. Note comparing to the controls, RBP-Jkappa cKO mouse PDL has delayed expression of Periostin at P10 and P14, but not at 2 months.

Bars: A, B, H-J: 20μm; C-F: 1mm.

Figure 4. Stretching force induced *Notch* pathway activation and matrix protein productions on a human PDL cell line.

A and B: Real time RT-PCR analysis on human PDL cells at a ratio of 20% stretching and frequency of 30x/min. Samples were collected after 12 hours. ** $p<0.01$.

C: Metacore analysis of proteomic analysis on the samples of A and B.

D: String analysis of the top 5 pathways affected by stretching force.

Figure 5. Lamin A is a marker of PDL maturation and is under the control of Notch pathway.

A: Compound analysis of the common targets from the *in vivo* RNAseq (Figure 1) and proteomic and *in vitro* cell stretching results (Figure 4). Note Lamin A (LMNA) is the only molecule that was commonly regulated in the three conditions.

B: Immunofluorescent analysis of Lamin A/C expression in the P18 vs. P28 PDL. D: Dentin; B: Bone; Dotted lines: boundaries.

C: Western blotting analysis of Lamin A/C expression in the human PDL cells upon stretching (Figure 4 A&B), with GapDH as the loading control. Note only Lamin A expression was significantly changed.

D: Western blotting analysis of Lamin A/C expression in the human PDL cells treated with Jagged1, with GapDH as the loading control. Note again only Lamin A expression was significantly changed.

E and F: Immunofluorescent analysis of Lamin A/C expression in the control and cKO mouse PDL at P10 and 2 months. D: Dentin; B: Bone; Dotted lines: boundaries.

Bars: 20μm

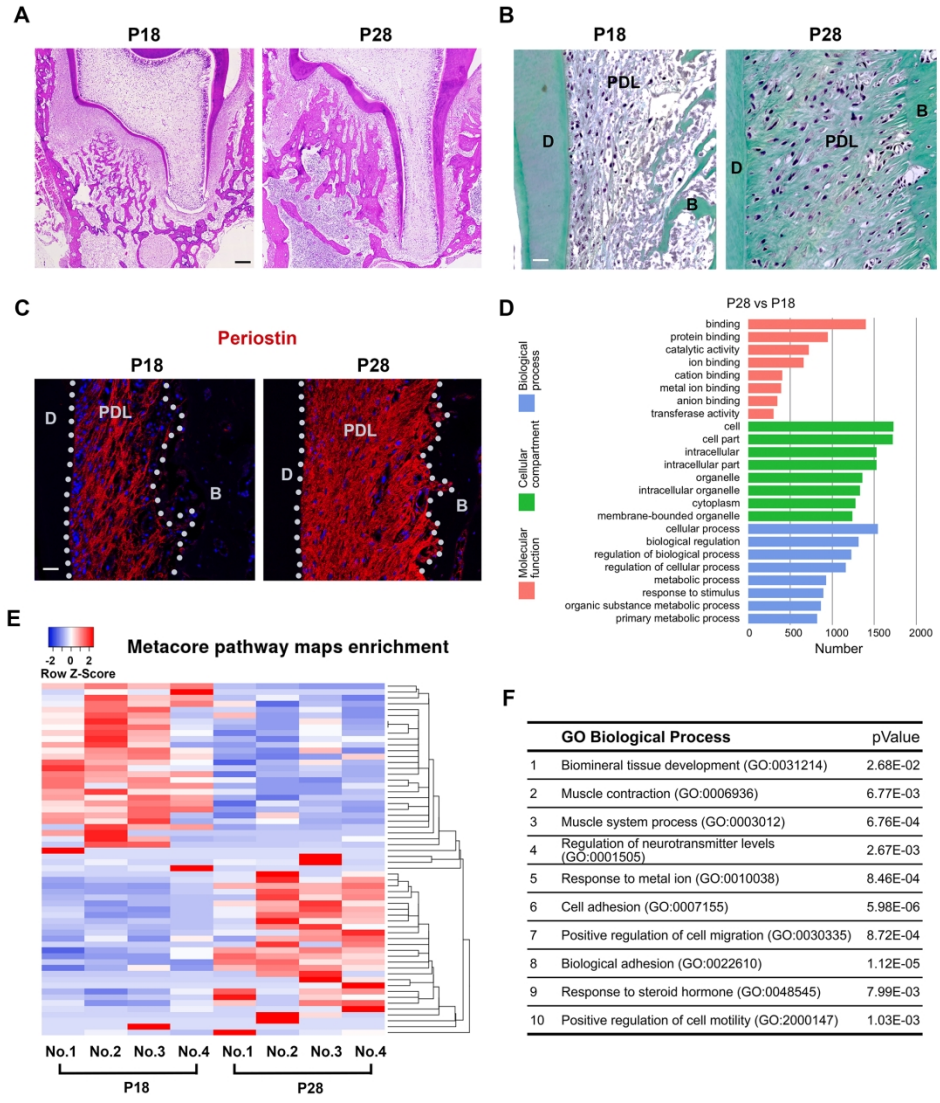

	GO Biological Process	pValue
1	Biomineral tissue development (GO:0031214)	2.68E-02
2	Muscle contraction (GO:0006936)	6.77E-03
3	Muscle system process (GO:0003012)	6.76E-04
4	Regulation of neurotransmitter levels (GO:0001505)	2.67E-03
5	Response to metal ion (GO:0010038)	8.46E-04
6	Cell adhesion (GO:0007155)	5.98E-06
7	Positive regulation of cell migration (GO:0030335)	8.72E-04
8	Biological adhesion (GO:0022610)	1.12E-05
9	Response to steroid hormone (GO:0048545)	7.99E-03
10	Positive regulation of cell motility (GO:2000147)	1.03E-03

Figure 1

182x227mm (300 x 300 DPI)

A

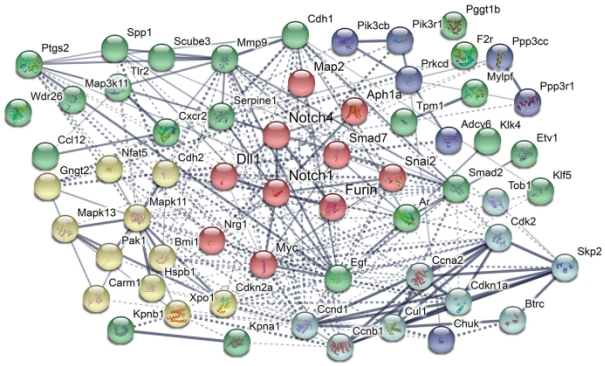

B

	Pathway Maps	pValue
1	PI3K signaling in gastric cancer	6.44E-08
2	Notch signaling in breast cancer	1.18E-07
3	Cell cycle - Nucleocytoplasmic transport of CDK/Cyclins	6.08E-07
4	Inhibition of TGF-beta 1 signaling in early colorectal cancer	3.59E-06
5	Cell cycle - Influence of Ras and Rho proteins on G1/S Transition	4.30E-06

C

Gene	Fold change	pValue
Notch1	2.08	0.011
Notch4	2.11	0.018
Dll1	7.19	0.031
Jag1	2.52	0.067
Furin	0.5	0.000

D

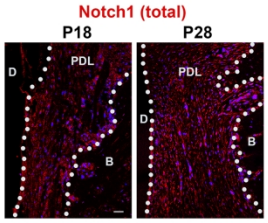

E

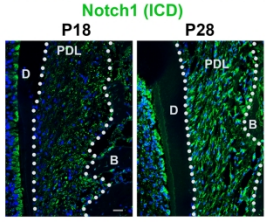

F

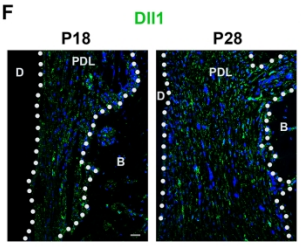

G

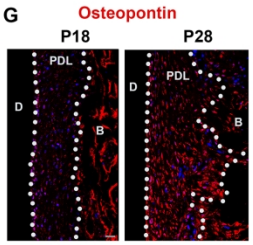

H

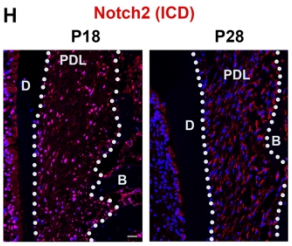

Figure 2

184x252mm (300 x 300 DPI)

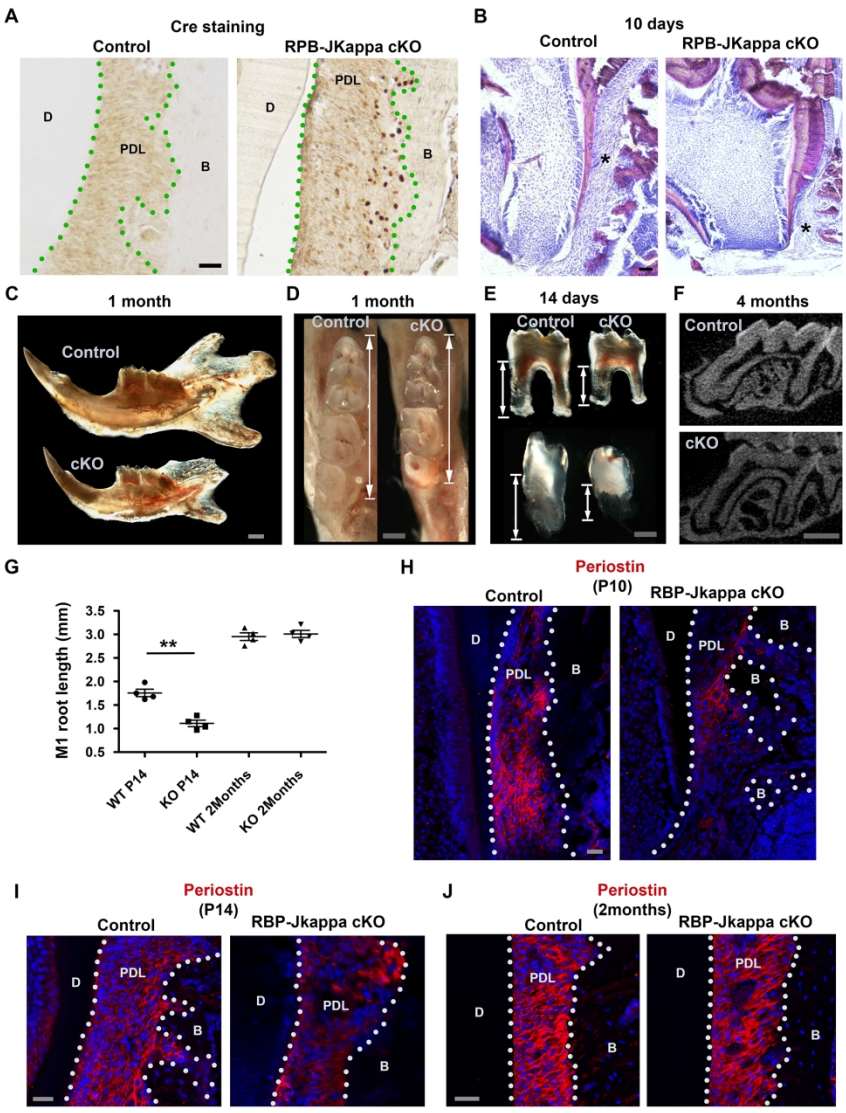
A
Cre staining
Control
RPB-JKappa cKO
D
PDL
B
B
10 days
Control
RPB-JKappa cKO
*
*
C
1 month
Control
cKO
D
1 month
Control
cKO
E
14 days
Control
cKO
F
4 months
Control
cKO
G
M1 root length (mm)
3.5
3.0
2.5
2.0
1.5
1.0
0.5
**
WT P14
KO P14
WT 2Months
KO 2Months
H
Periostin
(P10)
Control
RBP-Jkappa cKO
D
PDL
B
B
I
Periostin
(P14)
Control
RBP-Jkappa cKO
J
Periostin
(2months)
Control
RBP-Jkappa cKO

Figure 3

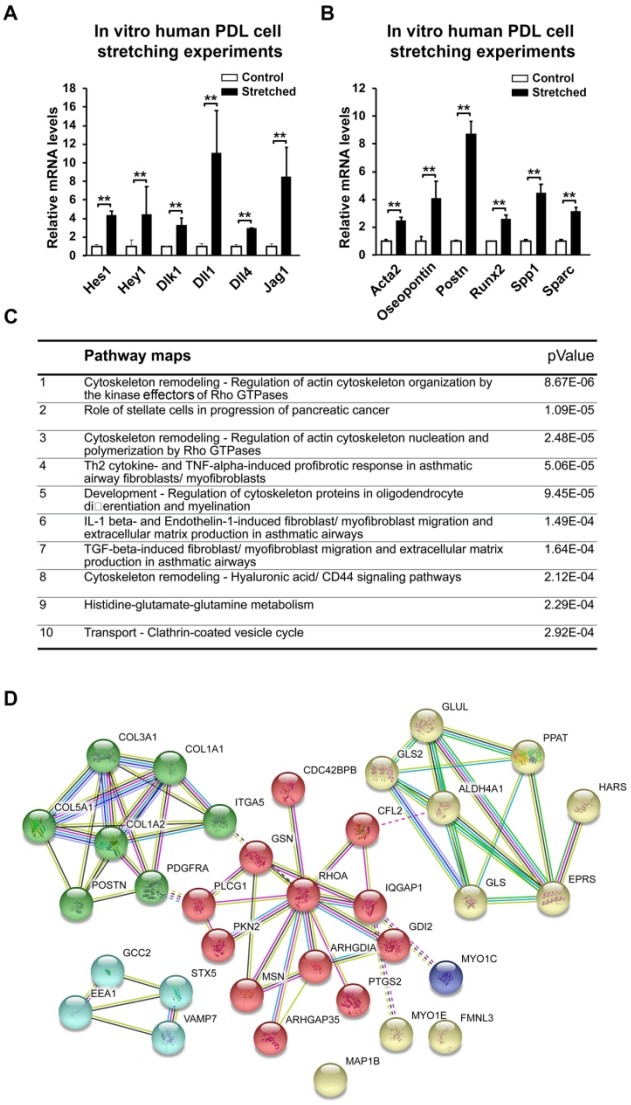

C

	Pathway maps	pValue
1	Cytoskeleton remodeling - Regulation of actin cytoskeleton organization by the kinase effectors of Rho GTPases	8.67E-06
2	Role of stellate cells in progression of pancreatic cancer	1.09E-05
3	Cytoskeleton remodeling - Regulation of actin cytoskeleton nucleation and polymerization by Rho GTPases	2.48E-05
4	Th2 cytokine- and TNF-alpha-induced profibrotic response in asthmatic airway fibroblasts/ myofibroblasts	5.06E-05
5	Development - Regulation of cytoskeleton proteins in oligodendrocyte differentiation and myelination	9.45E-05
6	IL-1 beta- and Endothelin-1-induced fibroblast/ myofibroblast migration and extracellular matrix production in asthmatic airways	1.49E-04
7	TGF-beta-induced fibroblast/ myofibroblast migration and extracellular matrix production in asthmatic airways	1.64E-04
8	Cytoskeleton remodeling - Hyaluronic acid/ CD44 signaling pathways	2.12E-04
9	Histidine-glutamate-glutamine metabolism	2.29E-04
10	Transport - Clathrin-coated vesicle cycle	2.92E-04

Figure 4

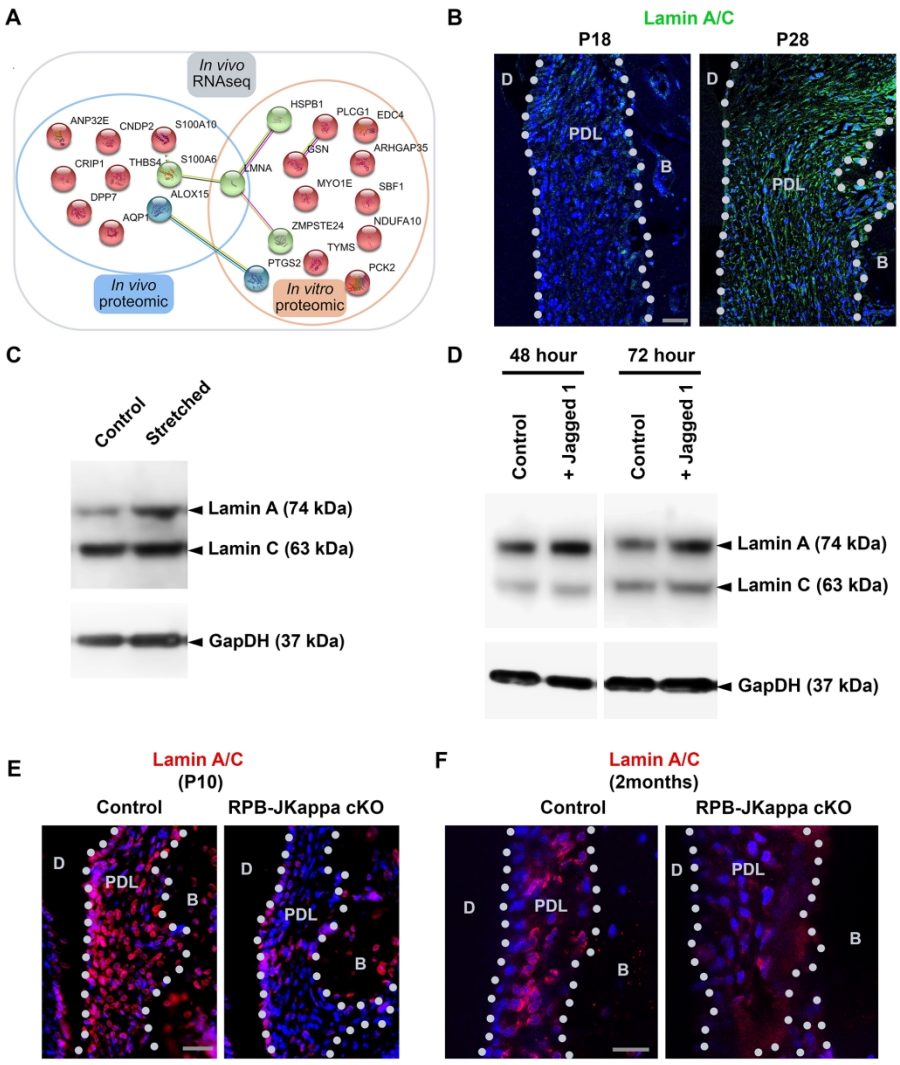

Figure 5

176x227mm (300 x 300 DPI)

Notch coordinates periodontal ligament maturation through regulating Lamin A

Balazs Jozsef Denes[1], Chloe Bolton[2], Charlotte Sara Illsley[2], Wai Ling Kok[2], Jemma Victoria Walker[2], Ansgar Poetsch[3], Christopher Tredwin[2], Stavros Kiliaridis[1], Bing Hu[2*]

Appendix files and legends

Appendix Figure 1

A: Additional micro-CT analysis on P18 and P28 rat root.

B: Additional process network analysis on the RNAseq results illustrated in Figure 1.

Bar: 100μm

Appendix Figure 2

A: Periostin expression analysis at postnatal day 4 (P4) in the control and RBP-Jkappa cKO mice.

B: The stretching device system used in this study.

Bar: 20μm

Appendix Figure 3

Summarisation of the findings of study and perspectives.

Appendix Table 1

The RNAseq summary of the study.

Appendix Table 2

The original proteomic analysis data of stretched PDL cells showed in Figure 4.

Appendix Table 3

The antibodies, primers and protein used in the study.

A

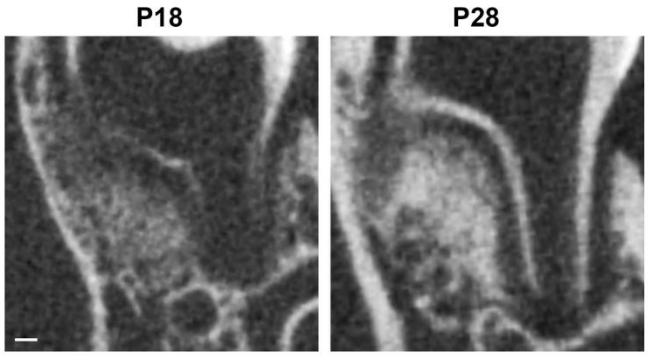

B

	Process networks	pValue
1	Development - Neurogenesis - Axonal guidance	2.80E-04
2	Development - Ossification and bone remodeling	3.14E-04
3	Muscle contraction	3.69E-04
4	Signal Transduction - TGF-beta, GDF and Activin signaling	5.06E-04
5	Cell adhesion - Cell junctions	5.47E-04
6	Cell cycle - G1-S Growth factor regulation	7.53E-04
7	Signal transduction - NOTCH signaling	8.64E-04
8	Inflammation - IFN-gamma signaling	9.05E-04
9	Development - Blood vessel morphogenesis	9.24E-04
10	Proliferation - Positive regulation cell proliferation	9.86E-04

Appendix Figure 1

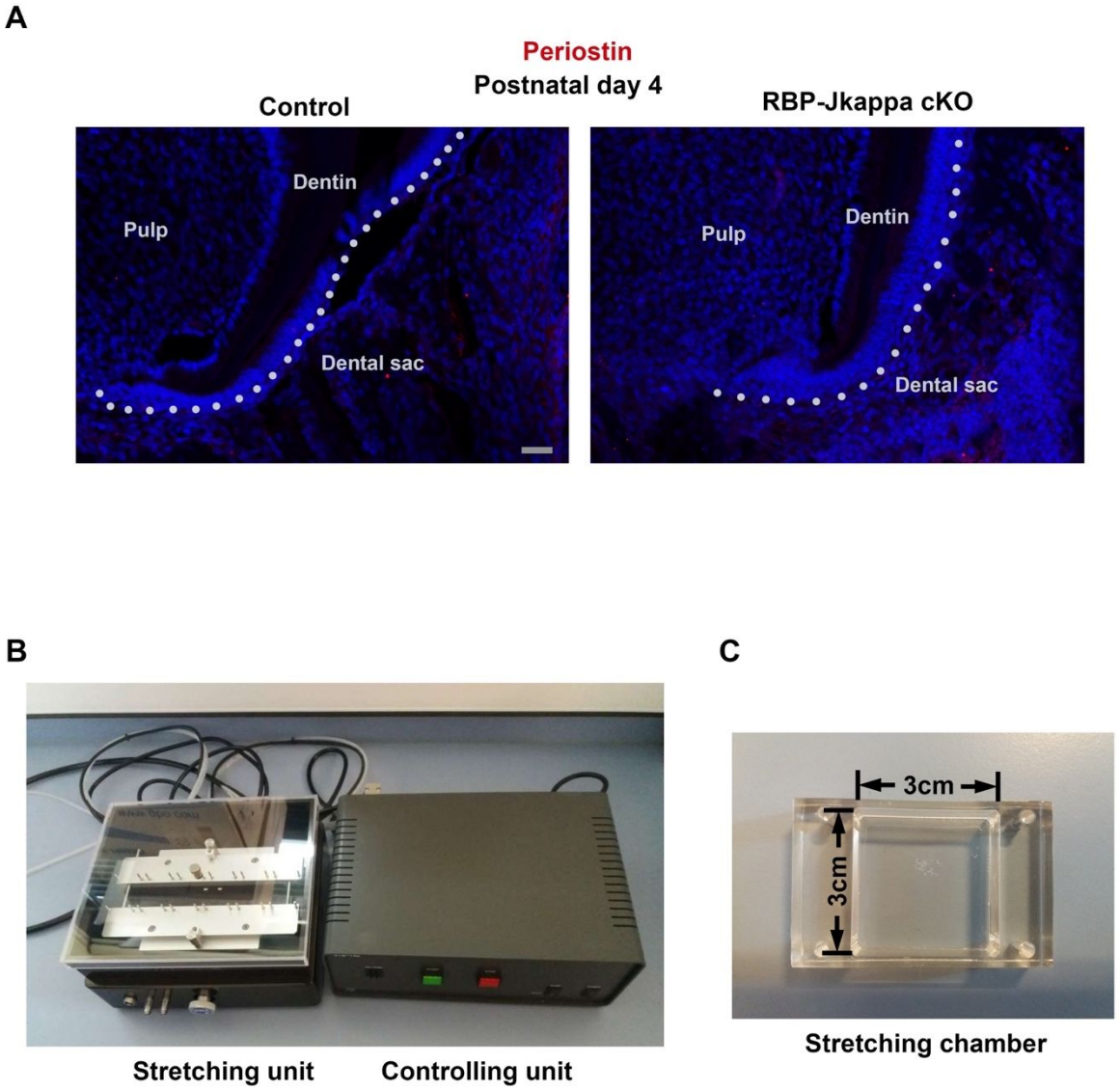

Appendix Figure 2

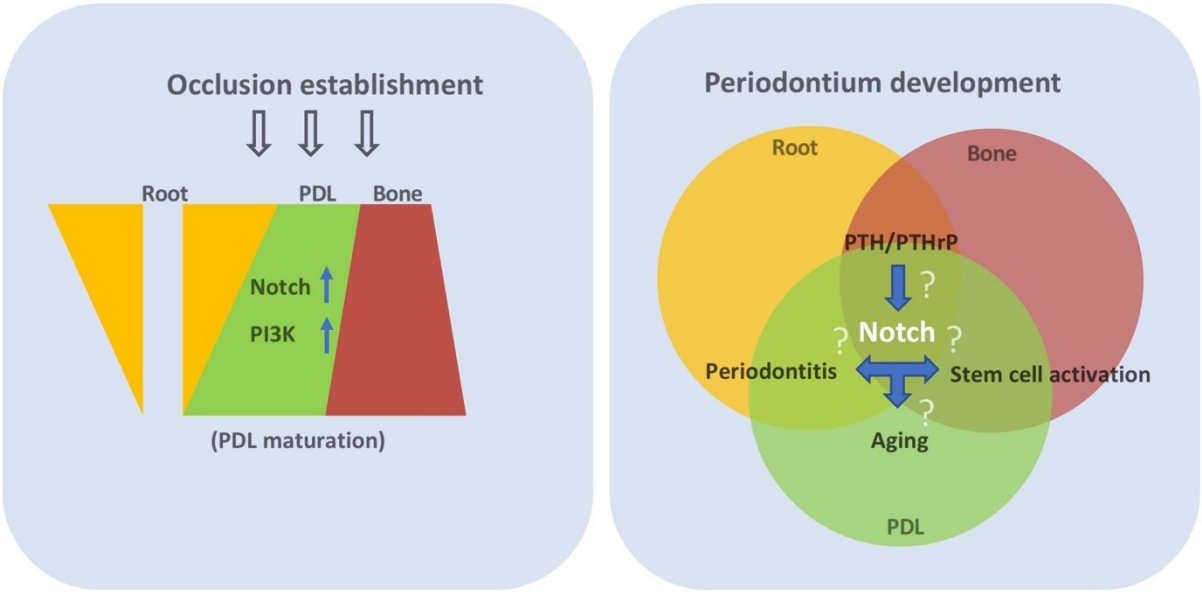

Appendix Figure 3

Appendix Table 1

Summary of the fold changes of the genes up and down regulated comparing P28 with P18 PDL based on the RNAseq analysis results as showed in Figure 1D. The genes inside the category of "Cell" has been shown as below.

A4galt	56.2	0.012
Aak1	-6.2	0.046
Aatf	-3.0	0.001
Abca2	4.4	0.001
Abca4	-27.3	0.034
Abca7	5.6	0.036
Abcc2	-29.1	0.037
Abcc5	2.9	0.006
Abcd3	2.5	0.023
Abce1	-2.0	0.001
Abi1	1.7	0.008
Abi3	2.6	0.005
Abt1	1.5	0.046
Acads	1.6	0.038
Acbd3	2.1	0.032
Acer1	60.2	0.042
Ache	-10.8	0.013
Ache	-10.8	0.013
Ackr2	840.3	0.003
Ackr3	2.7	0.006
Acot11	-122.2	0.039
Acox1	-5.4	0.016
Acp5	12.7	0.001
Acsbg1	77.1	0.038
Acta2	-4.2	0.004
Actr10	-1.6	0.022
Actr3	-1.9	0.017
Acvr1b	24.5	0.044
Adam19	-1.8	0.044
Adamts15	32.3	0.036
Adcy10	89.7	0.015
Adcy6	2.4	0.029
Adcyap1r1	23.1	0.022
Adh4	16.2	0.046
Adh5	-1.5	0.020
Adh6a	-126.0	0.020
Adh7	1517.8	0.003
Adm	-10.4	0.000
Adpgk	-1.6	0.016

Adra1b	28.5	0.032
Adrb1	-59.2	0.048
Adsl	-1.9	0.003
Afg3l2	-1.7	0.048
Aga	1.7	0.009
Agpat4	-2.3	0.002
Agps	-2.9	0.042
Ahnak	2.2	0.032
Aif1l	-8.4	0.016
Ak1	-1.9	0.015
Akap12	2.2	0.018
Akap17a	2.6	0.021
Akap5	-158.1	0.017
Akap8l	2.4	0.001
Akip1	1.9	0.013
Alad	-1.8	0.045
Alas2	-5.7	0.012
Aldh1a3	-73.2	0.017
Aldh1b1	-159.0	0.002
Aldh1l1	-9.6	0.031
Aldh6a1	-1.8	0.013
Alg11	-3.1	0.000
Alg2	-2.6	0.004
Alk	339.8	0.006
Alox15	-11.1	0.001
Als2	-11.3	0.032
Amelx	-88.0	0.006
Amigo1	-147.1	0.025
Ampd1	60.5	0.011
Amph	-19.5	0.036
Anapc1	-1.7	0.033
Anapc5	-1.6	0.001
Angptl6	49.7	0.023
Ankhd1	2.1	0.011
Ankrd13a	-1.8	0.010
Ankrd23	22.9	0.036
Anp32e	-2.7	0.000
Aox3	31.0	0.032
Ap1s2	-1.7	0.026
Ap2m1	-1.7	0.003
Aph1a	-2.3	0.001
Api5	-1.7	0.004
Apoc3	55.0	0.011
Aqp1	2.7	0.015
Aqp3	211.9	0.001
Aqp4	1752.4	0.001

Ar	20.5	0.005
Ar	20.5	0.005
Ar	20.5	0.005
Ar	20.5	0.005
Arcn1	-1.9	0.001
Arf1	-1.8	0.021
Arf2	-1.9	0.017
Arf4	-1.5	0.004
Arfip1	-2.6	0.007
Arfip2	2.3	0.003
Arg2	5.8	0.000
Arglu1	2.0	0.028
Arhgap35	1.9	0.047
Arhgap4	-4.8	0.027
Arhgef18	-1.9	0.037
Arhgef25	-1.8	0.013
Arhgef7	-1.7	0.037
Arl1	-2.6	0.001
Arl3	1.6	0.015
Arl6ip1	-1.6	0.050
Arntl	2.3	0.025
Arntl2	-85.0	0.036
Arrdc1	1.6	0.009
Arsi	7.2	0.019
Asgr2	178.3	0.002
Ash1l	2.0	0.039
Asic1	79.2	0.023
Asip	71.8	0.027
Atad1	-2.0	0.021
Ate1	1.9	0.016
Atf4	1.6	0.012
Atic	-2.8	0.000
Atl2	-4.1	0.031
Atoh8	3.6	0.001
Atp1a3	-52.7	0.032
Atp2a2	-1.6	0.010
Atp2b2	98.2	0.013
Atp2b3	36.5	0.049
Atp2b4	1.9	0.038
Atp5e	2.0	0.030
Atp5i	1.7	0.039
Atp5j2	1.7	0.029
Atp6v0b	2.4	0.001
Atp6v1e1	1.7	0.005
Atp6v1e2	164.2	0.017
Atp6v1f	1.8	0.001

Atxn10	-2.2	0.000
Avil	417.1	0.000
Avp	183.0	0.008
Azin2	5.5	0.028
B2m	2.0	0.002
B3galnt1	-1.6	0.040
B3galt1	-264.1	0.037
B3galt2	-43.4	0.012
B3galt6	-3.0	0.018
B3gat3	1.9	0.001
B4galnt4	-13.4	0.047
B4galt2	-1.6	0.014
B4galt6	1.9	0.008
B9d2	1.8	0.013
Bag3	1.8	0.042
Bag4	-4.3	0.031
Batf	3.3	0.017
Bbs2	-2.0	0.043
Bche	-122.2	0.031
Bckdhb	-1.9	0.003
Bcl2l15	42.5	0.050
Bcl6	4.9	0.002
Bcorl1	2.4	0.034
Bglap	4.6	0.003
Blk	-17.9	0.002
Bloc1s1	1.6	0.037
Blzf1	-2.2	0.036
Bmi1	-7.3	0.013
Bmpr1a	-3.8	0.006
Bmx	-30.0	0.013
Bod1	1.6	0.028
Brd9	1.7	0.043
Brf1	-1.7	0.037
Bri3	2.4	0.009
Brinp1	-42.1	0.000
Brinp2	121.9	0.003
Brms1l	-4.0	0.006
Btaf1	1.7	0.046
Btbd1	-1.7	0.009
Btbd6	-1.7	0.010
Btk	-7.5	0.014
Btnl2	-63.2	0.022
Btrc	-2.8	0.015
Bub1	-2.7	0.013
Bzw1	-2.2	0.011
Bzw2	-2.0	0.001

C1qa	2.5	0.003
C1qb	1.9	0.041
C1qc	1.9	0.042
Cacna1c	-4.9	0.004
Cacna2d4	30.2	0.045
Cacnb4	74.6	0.018
Cacng6	-137.5	0.026
Cadm1	4.0	0.003
Calb1	-39.7	0.008
Calcb	-65.3	0.023
Calm3	-1.5	0.037
Camk1g	146.8	0.018
Camk2a	-34.6	0.047
Camk2d	-4.3	0.031
Capg	2.9	0.001
Capn12	4.9	0.005
Capn15	2.6	0.026
Capn3	-348.3	0.001
Caprin1	-2.1	0.002
Capza1	-1.9	0.002
Capza2	-1.6	0.014
Carf	15.0	0.025
Carm1	-2.1	0.017
Casp1	-4.0	0.017
Casp4	3.4	0.006
Casp7	-3.6	0.008
Casp8	-11.9	0.000
Cav3	72.1	0.044
Cbll1	1.9	0.003
Cbx7	7.3	0.049
Ccar1	1.7	0.035
Ccdc22	3.9	0.024
Ccdc67	-170.7	0.012
Ccdc69	-20.1	0.032
Cchcr1	1.8	0.020
Ccl12	112.4	0.015
Ccl21	258.3	0.014
Ccna2	-3.1	0.006
Ccnb1	-2.1	0.026
Ccnb1ip1	427.6	0.003
Ccnd1	2.1	0.025
Ccndbp1	1.9	0.004
Ccnh	-1.7	0.015
Ccny	-1.9	0.042
Ccr7	44.0	0.046
Cct6a	-1.6	0.011

Cd164	-1.8	0.001
Cd177	-22.0	0.027
Cd19	-64.0	0.004
Cd22	-97.8	0.002
Cd244	-34.9	0.016
Cd320	1.8	0.008
Cd36	-10.9	0.017
Cd38	-22.3	0.027
Cd3g	-10.1	0.032
Cd44	1.9	0.029
Cd5	92.0	0.023
Cd55	17.0	0.009
Cd68	3.0	0.013
Cd69	-569.3	0.003
Cd79b	-6.2	0.017
Cd9	2.3	0.000
Cd99	2.0	0.014
Cdc123	-1.7	0.005
Cdc14a	3.2	0.013
Cdc16	-2.2	0.000
Cdc23	-2.0	0.011
Cdc26	-2.7	0.000
Cdc34	1.7	0.026
Cdc40	-1.8	0.028
Cdc6	-4.8	0.015
Cdca7	-3.2	0.011
Cdh1	8.6	0.046
Cdh13	2.5	0.002
Cdh17	62.4	0.004
Cdh2	2.9	0.031
Cdk2	-2.1	0.047
Cdk2ap2	1.9	0.001
Cdk5	2.3	0.001
Cdkn1a	5.1	0.004
Cdkn2a	-71.7	0.035
Cdkn2aip,Carf	#N/A	#N/A
Cdnf	273.1	0.012
Cdv3	2.1	0.020
Cebpd	-1.8	0.029
Cers3	67.1	0.031
Cfap126	-129.8	0.019
Cgnl1	7.2	0.001
Chchd10	5.9	0.041
Chi3l1	-17.2	0.006
Chp1	-2.0	0.036
Chpf2	-1.7	0.016

Chrna4	-12.6	0.022
Chrnb1	53.6	0.011
Chst11	11.2	0.039
Chst12	-1.7	0.035
Chuk	-2.3	0.011
Cidea	-247.0	0.012
Cideb	-27.2	0.032
Cited1	-39.0	0.035
Cited2	1.9	0.011
Ckb	2.1	0.024
Cks2	1.8	0.037
Clca5	155.2	0.008
Clcn3	-3.8	0.031
Cldn10	-443.2	0.001
Cldn20	-229.9	0.009
Cldnd1	-2.0	0.000
Clip4	24.3	0.048
Clk1	2.7	0.001
Cln3	2.9	0.013
Cln8	-2.8	0.011
Clock	2.6	0.030
Clstn1	1.7	0.049
Clstn3	424.9	0.001
Clu	-1.9	0.018
Clvs1	1.9	0.042
Clvs2	-76.4	0.041
Cmc1	2.1	0.006
Cmpk1	-1.7	0.001
Cndp2	-2.7	0.002
Cnep1r1	-2.2	0.026
Cnih2	-2.8	0.018
Cnn3	-1.6	0.016
Cnot10	2.1	0.003
Cnp	-1.8	0.016
Cnp	-1.8	0.016
Cnrip1	-1.7	0.032
Cntf	25.6	0.000
Cntn1	115.3	0.009
Cntn6	361.2	0.003
Cntnap4	1391.6	0.001
Coa4	2.0	0.007
Coasy	1.9	0.039
Cog4	-1.5	0.021
Cog6	-4.5	0.041
Cog7	-2.2	0.017
Col26a1	-3.6	0.017

Col4a3bp	3.3	0.028
Col6a2	2.0	0.007
Commd4	1.9	0.003
Copg1	-2.1	0.022
Coprs	1.9	0.014
Cops4	-2.1	0.001
Copz1	-1.5	0.004
Coq10b	-2.1	0.028
Coro1a	-3.0	0.017
Coro2a	144.1	0.004
Cotl1	-1.7	0.021
Cox17	1.9	0.012
Cox20	1.7	0.029
Cox7b	2.0	0.013
Cpeb1	276.3	0.015
Cpne9	33.9	0.026
Cpq	1.6	0.032
Cpsf4	-2.1	0.038
Cpt1c	3.3	0.037
Cr2	-201.2	0.009
Creb3l4	186.5	0.009
Crebbp	1.7	0.049
Crip1	2.5	0.002
Crip2	1.7	0.009
Crlf3	-4.8	0.003
Crls1	-2.0	0.023
Crtac1	49.4	0.020
Cs	-1.8	0.010
Csf2ra	3.7	0.000
Csnk1d	-1.6	0.003
Cspg4	2.8	0.012
Csrp2	-1.7	0.033
Cst3	2.9	0.000
Cstb	1.8	0.021
Cstf1	-2.7	0.000
Cstf2	-2.8	0.045
Ctbs	1.7	0.042
Ctdsp1	1.8	0.002
Ctdspl2	-2.4	0.024
Ctif	33.6	0.034
Ctps1	-2.5	0.000
Ctrb1	98.1	0.013
Ctsc	-2.7	0.008
Ctsd	1.7	0.001
Ctse	-26.6	0.000
Ctsf	1.7	0.021

Ctsw	-76.8	0.003
Ctsz	3.6	0.004
Cuedc2	1.6	0.029
Cul1	-2.9	0.000
Cul2	-1.8	0.049
Cul3	-1.6	0.018
Cxcl1	305.7	0.011
Cxcl10	136.2	0.021
Cxcl14	-2.0	0.044
Cxcr2	-43.8	0.035
Cxcr3	30.2	0.042
Cxcr6	-226.8	0.025
Cyb5b	-1.6	0.034
Cyba	1.7	0.018
Cyfip2	-7.9	0.002
Cyp27a1	9.7	0.038
Cyp27b1	163.4	0.019
Cyp2j10	220.6	0.001
Cyp2r1	45.8	0.022
Cyp39a1	283.3	0.005
Cyp3a9	92.3	0.031
Cyp4b1	206.1	0.008
Cyp7b1	-5.8	0.003
Cysltr1	-103.8	0.039
Dab2	-1.7	0.027
Dab2ip	1.9	0.016
Dapk1	2.0	0.023
Dars	-2.4	0.013
Dbf4	-3.8	0.039
Dbn1	-1.5	0.045
Dcaf8	-1.8	0.002
Dcdc2	93.5	0.031
Dcps	-2.6	0.008
Dcxr	2.2	0.010
Ddx46	1.6	0.027
Ddx50	-1.6	0.037
Ddx58	3.8	0.022
Ddx59	2.1	0.025
Dffa	2.2	0.005
Dgkg	-15.8	0.028
Dgki	298.6	0.000
Dhcr24	-35.7	0.002
Dhps	-2.1	0.002
Dhrs7c	145.1	0.018
Dhx30	2.1	0.006
Dhx8	-2.6	0.013

Dkkl1	-98.4	0.045
Dlgap4	2.1	0.002
Dll1	7.2	0.031
Dnaja3	-1.8	0.043
Dnajb13	263.7	0.002
Dnajb4	-2.1	0.016
Dnajb6	-2.1	0.015
Dnajc16	-900.3	0.000
Dnase1l1	2.9	0.011
Dnase1l3	-299.8	0.002
Dnase2	1.9	0.001
Dnase2b	44.0	0.019
Dnlz	1.9	0.021
Dnm3	-3.3	0.043
Dock8	-4.2	0.028
Dock9	2.9	0.034
Dpep1	29.8	0.039
Dpf1	92.0	0.001
Dph3	1.6	0.033
Dpp4	-19.8	0.004
Dpp7	1.8	0.010
Dpyd	84.5	0.003
Dpysl2	2.1	0.018
Dram2	-1.9	0.026
Drg1	-2.3	0.006
Dsc3	91.8	0.005
Dsg3	21.5	0.038
Duox1	3.7	0.011
Dusp10	-2.6	0.048
Dusp3	1.9	0.005
Dusp4	-33.4	0.038
Dvl1	2.1	0.012
Dym	-2.0	0.011
Dync1i2	1.5	0.047
Dyrk2	2.0	0.009
Eaf2	-36.5	0.041
Edar	-74.6	0.045
Edc4	2.1	0.003
Eef1a1	-1.9	0.018
Eef1e1	-2.1	0.003
Efemp1	5.1	0.037
Egf	22.1	0.036
Egfl7	1.9	0.012
Egr2	653.0	0.001
Ehf	187.0	0.020
Ehmt1	-5.3	0.001

Ei24	-2.2	0.000
Eif2b1	-1.6	0.011
Eif2b3	-2.5	0.003
Eif2s1	-1.6	0.018
Eif4a1	-1.5	0.002
Eif4e	-1.6	0.025
Elf1	-2.8	0.016
Elf4	-8.8	0.042
Elovl4	-6.4	0.012
Elovl5	-3.4	0.045
Emc4	1.7	0.002
Emd	2.1	0.020
Emid1	-2.9	0.000
Eml1	-3.1	0.020
Enc1	-3.1	0.010
Enoph1	-2.0	0.028
Enpp1	-2.5	0.018
Enpp2	3.1	0.020
Enpp6	130.7	0.001
Eogt	-23.6	0.015
Epc1	2.5	0.046
Epha1	233.9	0.003
Epha2	2.1	0.009
Erh	-1.6	0.001
Espn	30.6	0.008
Esrp1	73.2	0.017
Esrp2	130.5	0.025
Etf1	-1.5	0.030
Etv1	3.9	0.032
Eva1a	-1.8	0.027
Evpl	203.0	0.010
Exoc6b	-3.4	0.003
Ezh1	3.7	0.009
F11r	-1.8	0.047
F12	-154.6	0.010
F2r	-2.8	0.001
Fa2h	25.3	0.037
Fabp5	2.7	0.015
Fah	5.6	0.007
Fam118b	-2.1	0.045
Fam126a	-22.4	0.000
Fam126b	4.2	0.035
Fam161a	-82.9	0.016
Fam172a	-2.0	0.025
Fam20c	3.1	0.003
Fam26e	-15.4	0.041

Fam26f	25.2	0.039
Fam46c	-2.4	0.032
Fam65a	1.9	0.010
Fam96b	1.7	0.010
Fam98c	1.7	0.021
Fanca	4.9	0.003
Farsb	-3.9	0.000
Fasn	1.7	0.039
Fat1	2.3	0.036
Fbxl4	-4.1	0.024
Fbxl5	-1.7	0.042
Fbxo2	204.6	0.026
Fbxo39	42.3	0.042
Fbxo44	214.6	0.016
Fbxo7	-2.0	0.033
Fcmr	-5.2	0.020
Fcnb	-13.2	0.012
Fcrla	-6.4	0.049
Fdx1	1.6	0.010
Fem1a	1.8	0.003
Fermt1	5.8	0.036
Fgd4	37.1	0.009
Fgf9	57.2	0.022
Fgfbp1	1831.0	0.002
Fgfrl1	3.0	0.007
Fhl2	-2.3	0.015
Fhod1	4.1	0.006
Fibp	1.5	0.005
Flrt1	123.3	0.010
Flrt3	-3.5	0.025
Flt3	27.8	0.023
Fmr1	2.1	0.006
Fndc3a	3.3	0.002
Fnip1	2.7	0.008
Fnip2	23.1	0.007
Folh1	-151.6	0.044
Folr2	3.5	0.010
Foxi3	45.4	0.037
Foxj1	109.3	0.021
Foxk1	-3.7	0.040
Foxo3	2.2	0.015
Foxo4	6.1	0.024
Fpr1	-282.3	0.003
Frmd3	-143.3	0.027
Fscn3	531.0	0.006
Fsd1	-242.3	0.011

Fto	-5.3	0.004
Fundc2	1.6	0.015
Furin	-2.0	0.000
Fut11	-2.8	0.037
Fut7	215.2	0.003
Fut8	-5.7	0.000
Fxyd1	1.8	0.038
Fxyd2	6.8	0.000
Fxyd3	5.4	0.034
G3bp1	-1.9	0.002
G3bp2	-4.0	0.024
Gabarapl1	1.8	0.003
Gabbr1	2.9	0.007
Gabbr2	533.6	0.004
Gabrd	39.1	0.019
Gadd45g	1.8	0.021
Gale	2.5	0.017
Galm	2.2	0.037
Galnt1	-3.2	0.009
Galnt10	-4.4	0.002
Galt	1.6	0.050
Gatad2b	2.9	0.019
Gatm	-2.7	0.009
Gba2	1.8	0.034
Gc	-122.8	0.017
Gcgr	27.5	0.025
Gcn1l1	1.8	0.040
Gfi1	-52.5	0.017
Ggps1	-2.7	0.014
Ghr	-2.0	0.005
Ghrl	19.6	0.042
Gimap4	2.6	0.024
Gimap7	-12.6	0.028
Gjb2	43.7	0.022
Gjb3	131.2	0.027
Gjc1	-2.6	0.004
Gldn	23.6	0.035
Glrb	-70.6	0.008
Glrx	-2.4	0.001
Gls	1.8	0.018
Gls	1.8	0.018
Gmnn	-2.6	0.009
Gmppa	1.8	0.006
Gmppb	-2.8	0.000
Gmps	-1.7	0.029
Gnai3	-1.5	0.012

Gnal	-1.7	0.018
Gnb1	-1.6	0.014
Gngt2	2.3	0.013
Gnl2	-2.5	0.005
Gnl3	-1.5	0.019
Gnpda2	-2.9	0.028
Gnpnat1	-2.2	0.003
Golga1	3.8	0.003
Golga7	-1.9	0.026
Golt1b	-1.7	0.040
Gorasp2	-1.5	0.043
Gpc1	1.7	0.030
Gpc3	-10.5	0.000
Gpc4	-1.7	0.043
Gpcpd1	-2.6	0.002
Gpnmb	3.1	0.033
Gpr174	58.6	0.010
Gprc5a	65.2	0.021
Gpsm2	-2.5	0.001
Grb10	-1.8	0.029
Grik4	108.0	0.005
Grin2c	-84.4	0.049
Grm7	64.4	0.029
Grsf1	-1.8	0.001
Gsn	2.1	0.001
Gsr	-2.1	0.014
Gstk1	2.2	0.020
Gstm5	-1.8	0.012
Gtpbp2	3.1	0.000
Haao	-139.1	0.014
Hadh	-2.5	0.044
Hat1	-2.6	0.000
Havcr2	-327.5	0.027
Hbp1	-2.1	0.002
Hcfc1r1	1.7	0.017
Hdac1	-1.6	0.018
Hdac10	2.5	0.036
Hdac2	-1.8	0.000
Hexa	1.7	0.005
Hexim2	-2.2	0.016
Hgfac	265.0	0.011
Hibadh	-2.2	0.013
Hif1a	-1.9	0.002
Higd1a	1.6	0.031
Hint2	2.1	0.007
Hip1	2.0	0.014

Hipk2	3.7	0.031
Hist1h2bh	2.1	0.012
Hist1h4m,Hist1h4b	#N/A	#N/A
Hivep1	3.1	0.019
Hivep3	-4.9	0.028
Hmgcl	2.1	0.010
Hmgn2	-2.3	0.000
Hnrnpa2b1	-1.8	0.017
Hnrnpdl	-1.6	0.020
Hnrnpf	-1.8	0.030
Hnrnph2	-2.2	0.033
Hnrnpu	-1.5	0.002
Hoxb4	-27.5	0.042
Hoxd4	6.8	0.031
Hoxd9	31.9	0.044
Hp	-3.3	0.036
Hpd	-110.3	0.027
Hras	1.6	0.027
Hrh1	-260.9	0.025
Hrh3	-311.0	0.011
Hrk	66.4	0.032
Hsd17b14	97.6	0.023
Hsd17b8	2.4	0.001
Hsdl2	-1.9	0.045
Hsf2	-2.2	0.028
Hspa1l	128.5	0.022
Hspa5	-1.7	0.002
Hspb1	4.6	0.000
Hsph1	2.1	0.013
Htr1b	-87.1	0.027
Htr2b	50.1	0.015
Htr7	-107.7	0.027
Ica1	2.9	0.024
Icam4	-322.7	0.009
Icam5	30.9	0.034
Idh3a	-1.9	0.012
Ifi27	1.9	0.013
Ifi27l2b	7.6	0.000
Ifngr2	1.7	0.014
Ift57	-1.8	0.004
Igbp1	1.9	0.030
Igfbp6	54.1	0.000
Ikbip	-2.7	0.002
Il11	83.2	0.026
Il16	-10.1	0.000
Il1rl1	-27.1	0.021

Il3ra	2.5	0.020
Ilf2	-1.8	0.017
Ilf3	1.6	0.033
Impa1	-2.2	0.001
Ina	-32.5	0.035
Ing4	1.6	0.007
Inha	6.7	0.009
Inhba	3.1	0.026
Ino80	2.5	0.039
Insc	-2.0	0.030
Insig2	1.9	0.029
Insl3	143.6	0.017
Ip6k1	-2.8	0.015
Ireb2	-2.6	0.041
Irf3	1.9	0.011
Irgm	4.3	0.012
Irx2	51.0	0.008
Irx6	198.9	0.005
Isoc1	-2.5	0.001
Itch	-3.9	0.027
Itga10	5.5	0.001
Itga11	-2.9	0.009
Itga4	-9.7	0.005
Itga8	28.9	0.021
Itgae	1.8	0.039
Itgb1bp2	66.9	0.017
Itgb4	3.1	0.009
Itgb6	142.4	0.013
Itm2a	-2.4	0.002
Itpka	300.2	0.010
Itpkb	-8.6	0.023
Itsn1	-3.2	0.020
Jade3	-536.5	0.002
Jmjd1c	1.9	0.011
Jmjd8	1.7	0.006
Junb	1.9	0.010
Kank1	3.9	0.017
Kars	-1.6	0.007
Kat7	-1.8	0.049
Kcna1	149.8	0.018
Kcna2	-182.6	0.045
Kcna3	-92.5	0.043
Kcnab3	108.8	0.007
Kcng1	-338.6	0.005
Kcnj12	122.8	0.039
Kcnj15	93.7	0.021

Kcnj9	86.0	0.016
Kcnmb4	3.1	0.001
Kcnq1	126.4	0.021
Kcnrg	-178.6	0.005
Kctd1	1.9	0.033
Kctd3	-3.3	0.001
Kdelc2	-1.7	0.049
Kdm1a	-1.7	0.003
Kdm4c	-11.3	0.000
Kdm8	2.0	0.038
Keap1	1.8	0.007
Kif19	72.2	0.037
Kif1c	2.7	0.030
Kif26b	-4.6	0.030
Kif27	-91.5	0.016
Kifc2	15.4	0.039
Kit	-33.8	0.013
Klf1	-30.1	0.002
Klf13	1.9	0.004
Klf16	-2.1	0.004
Klf3	1.7	0.007
Klf4	6.5	0.000
Klf5	4.5	0.026
Klhdc10	-3.3	0.040
Klhdc3	-1.8	0.001
Klhl14	-25.3	0.037
Klhl22	-1.6	0.034
Klhl40	209.8	0.026
Klhl41	145.5	0.015
Klhl8	2.1	0.034
Klhl9	-1.7	0.011
Klk4	-2388.5	0.004
Klk8	115.4	0.021
Klk8	115.4	0.021
Klrk1	-114.8	0.025
Kmt2e	1.8	0.002
Kpna1	-2.5	0.047
Kpnb1	-2.4	0.010
Krt10	2.4	0.034
Krt15	366.7	0.013
Krt17	21.1	0.033
Krt80	611.8	0.008
Ksr1	-6.0	0.011
L3mbtl2	2.0	0.035
Lamtor2	1.7	0.011
Lamtor4	1.7	0.009

Lancl2	-4.1	0.036
Laptm4b	-2.0	0.000
Larp6	3.8	0.002
Lbr	-3.2	0.032
Lbr	-3.2	0.032
Ldah	-3.1	0.003
Ldb2	2.5	0.010
Leprot	1.7	0.004
Lgals3	5.3	0.000
Lgals7	165.8	0.002
Lgr5	390.4	0.014
Lime1	13.5	0.004
Lims1	-2.3	0.001
Liph	105.6	0.024
Litaf	1.8	0.003
Lix1l	2.2	0.006
Llgl1	-2.0	0.003
Lmbr1l	2.7	0.041
Lmf2	2.0	0.000
Lmna	1.5	0.033
Lmnb1	-3.1	0.017
LOC100302465	-164.2	0.023
Lpar6	-1.7	0.050
Lpp	2.3	0.030
Lrfn4	1.8	0.030
Lrrc1	-4.4	0.044
Lrrc29	255.4	0.001
Lrrc46	802.5	0.001
Lrrc4b	2.6	0.031
Lrrc59	-1.6	0.048
Lrrn3	-19.7	0.036
LRRTM1	-28.4	0.007
Lsm14a	-1.5	0.031
Lsm8	1.6	0.025
Lss	-10.1	0.001
Lst1	-5.0	0.010
Lta4h	-1.8	0.030
Ltbp1	2.8	0.001
Ltv1	-1.9	0.012
Luc7l	2.2	0.001
Ly6d	840.4	0.000
Ly6g6f	-78.6	0.028
Lynx1	835.0	0.020
Lypd3	12.4	0.022
Lypla1	-2.1	0.003
Magt1	-3.6	0.000

Mal2	113.9	0.010
Mamdc4	73.4	0.016
Man1a1	-3.6	0.027
Maoa	-2.4	0.033
Map2	-25.9	0.033
Map2	-25.9	0.033
Map3k11	2.1	0.040
Map4k1	-3.2	0.012
Map4k4	2.4	0.022
Mapk11	139.4	0.017
Mapk13	64.3	0.007
Mapre1	-1.6	0.009
Mapt	20.7	0.042
Marc1	4.3	0.036
March2	2.3	0.000
March3	-4.1	0.015
March5	-2.2	0.010
March7	-7.2	0.000
Matk	4.5	0.026
Mbip	-2.5	0.020
Mcc	21.3	0.027
Mccc1	-2.5	0.049
Mccc2	-1.9	0.048
Mcfd2	-1.9	0.001
Mcl1	-1.6	0.026
Mcm10	-43.8	0.000
Mcm2	-2.8	0.005
Mcm4	-2.1	0.010
Mcm6	-2.6	0.017
Mcoln3	75.4	0.014
Mcpt2	-421.7	0.003
Mdfic	1.7	0.043
Mdk	-1.7	0.031
Me3	131.8	0.003
Mea1	1.6	0.014
Med13	2.3	0.006
Med15	1.7	0.003
Med19	1.7	0.029
Med20	-2.0	0.009
Med31	1.8	0.002
Mef2b	-53.1	0.047
Mei4	-137.5	0.028
Mest	-6.6	0.000
Mettl23	1.8	0.030
Mettl4	-12.7	0.025
Mfsd12	-26.6	0.014

Mgarp	341.5	0.005
Mgp	2.2	0.034
Mgrn1	-2.8	0.006
Mid1ip1	2.3	0.023
Mina	-3.0	0.001
Mios	-2.9	0.001
Mis12	-2.5	0.022
Mknk2	-1.6	0.020
Mlana	35.3	0.001
Mlph	76.0	0.020
Mmgt1	-2.8	0.049
Mmp23	-1.8	0.038
Mmp24	2.2	0.019
Mmp3	107.3	0.012
Mok	4.7	0.036
Morc1	-58.8	0.038
Morf4l2	-1.7	0.001
Mospd4	146.2	0.013
Mpc2	1.9	0.008
Mpg	1.6	0.040
Mpp6	-1.9	0.015
Mprip	-1.5	0.015
Mpv17l2	1.7	0.022
Mpzl2	21.1	0.023
Mrc1	1.8	0.031
Mri1	2.8	0.004
Mrpl14	1.6	0.022
Mrpl32	1.7	0.009
Mrpl54	1.8	0.041
mrpl9	2.1	0.001
Mrps2	-2.0	0.026
Mrps22	1.8	0.049
Mrps27	-2.2	0.049
Mrps30	-1.8	0.025
Ms4a1	-12.6	0.014
Ms4a2	-40.1	0.014
Msl1	1.7	0.006
Mst1r	41.7	0.049
Msto1	2.2	0.047
Mt1a	7.5	0.000
Mt3	60.7	0.000
Mt4	1334.1	0.003
Mta2	-1.7	0.015
Mterfd1	-2.2	0.000
Mtf2	-1.6	0.041
Mtmr2	-1.8	0.048

Mtmr7	-52.9	0.020
Mto1	3.2	0.037
Mtrr	2.7	0.017
Muc1	233.8	0.004
Muc20	-445.1	0.007
Mvb12a	1.9	0.002
Mx2	229.4	0.010
Mybl1	80.7	0.010
Myc	-2.0	0.001
Mycbp2	2.1	0.028
Myh10	-1.6	0.043
Myl1	1233.0	0.003
Mylpf	6.6	0.043
Myo1d	3.0	0.001
Myo1e	2.6	0.043
Myo7a	30.1	0.045
Myo9a	3.3	0.006
Myoc	155.0	0.011
Myof	2.5	0.019
Myom2	706.7	0.004
Mzb1	-17.6	0.021
N4bp2l2	1.7	0.008
Nadk2	-3.7	0.010
Nags	82.2	0.006
Ncaph2	-2.0	0.012
Ncbp1	-1.9	0.003
Ncf2	-117.9	0.014
Ncoa5	-2.6	0.000
Ndel1	-1.6	0.033
Ndfip2	-1.9	0.004
Ndufa10	-1.7	0.004
Ndufaf1	-9.7	0.006
Ndufs5	2.3	0.003
Nek6	-4.0	0.000
Neto2	-5.7	0.046
Neu3	25.5	0.012
Nfat5	2.1	0.047
Nfatc1	1.7	0.017
Nfil3	-2.3	0.019
Nfkbia	1.5	0.002
Nfkbiz	6.4	0.011
Nfx1	-2.6	0.001
Ngp	-19.0	0.011
Nin	6.7	0.003
Nkx2-3	67.5	0.028
Nkx6-3	94.9	0.009

Nmbr	49.8	0.044
Nmnat2	70.0	0.026
Nmur1	-108.6	0.030
Nnat	4.5	0.000
Nnt	-1.5	0.017
Nob1	1.7	0.011
Noc2l	-3.1	0.001
Nod2	23.3	0.037
Nol10	-2.4	0.019
Nop56	-1.7	0.033
Nop58	-1.5	0.028
Nos1	41.0	0.035
Nos2	63.9	0.025
Notch1	2.1	0.011
Notch4	2.1	0.018
Npas2	5.5	0.010
Npc1	3.0	0.003
Nphs1	67.9	0.027
Npr3	-423.3	0.014
Nptn	1.6	0.005
Npy4r	-131.4	0.035
Npy5r	64.0	0.040
Nr0b2	416.4	0.002
Nr1h2	1.7	0.002
Nr2c1	-2.3	0.017
Nr4a1	2.4	0.047
Nras	-2.2	0.047
Nrg1	103.2	0.011
Nrg1	103.2	0.011
Nrg2	-8.5	0.043
Nrp2	-2.2	0.042
Nrxn1	-5.6	0.039
Nsg1	-1.9	0.022
Nsmce4a	-1.7	0.014
Nsun2	-2.3	0.001
Nt5c1b	-70.8	0.048
Ntmt1	1.6	0.005
Ntn3	-3.0	0.048
Nuak2	14.4	0.027
Nudt17	342.1	0.005
Nufip1	-2.1	0.013
Numa1	2.0	0.003
Nup35	-1.8	0.034
Nup62	-2.1	0.003
Nup93	-1.9	0.012
Nupl1	-5.9	0.004

Nus1	-1.8	0.010
Oas3	81.3	0.017
Oat	-1.6	0.001
Ogdhl	13.2	0.014
Ogdhl,Ogdh	#N/A	#N/A
Ogfr	1.7	0.004
Olfm4	-16.4	0.045
Ormdl2	2.1	0.001
Ormdl3	-1.9	0.044
Ovol1	120.7	0.009
P2rx3	-14.2	0.038
P2ry2	2.8	0.047
P4ha3	-3.4	0.004
Pafah1b2	-3.0	0.000
Pafah2	-104.0	0.004
Pak1	-3.7	0.001
Pak3	-4.6	0.039
Palmd	3.5	0.006
Palmd	3.5	0.006
Pam16	1.9	0.024
Pam16	1.9	0.024
Pard3b	2.4	0.024
Pard6g	-2.8	0.000
Parl	-1.6	0.015
Parvg	-41.7	0.009
Pax8	724.6	0.001
Paxip1	-2.0	0.039
Pc	-2.9	0.018
Pc	-2.9	0.018
Pccb	-1.8	0.006
Pcdh18	-2.2	0.033
Pcdh9	-11.9	0.001
Pcdhga8	55.3	0.029
Pck2	1.9	0.005
Pcmtd1	1.6	0.025
Pcmtd2	1.6	0.044
Pcsk1	1275.4	0.000
Pcsk1	1275.4	0.000
Pde10a	411.1	0.001
Pde1b	-291.6	0.018
Pde4dip	-2.1	0.006
Pdia4	-1.9	0.001
Pdia6	-2.2	0.000
Pdk1	-1.8	0.015
Pdk1	-1.8	0.015
Pdlim2	2.2	0.012

Pdlim5	-3.2	0.002
Pdpr	-235.7	0.002
Pdxp	-3.2	0.000
Pdzd2	4.2	0.014
Pdzd7	175.7	0.025
Pecam1	1.9	0.014
Peg3	-2.0	0.029
Peg3	-2.0	0.029
Peli1	-2.4	0.027
Penk	-2.4	0.020
Per3	-3.8	0.034
Pet100	1.6	0.037
Pex11b	-2.5	0.028
Pex13	-1.7	0.022
Pex16	2.3	0.001
Pex26	4.3	0.005
Pex6	2.0	0.042
Pex7	-8.9	0.001
Pfdn6	2.0	0.049
Pgam2	-21.0	0.036
Pgbd5	-410.6	0.008
Pggt1b	-3.7	0.014
Pgp	1.5	0.023
Phb2	-1.5	0.005
Phkg1	134.3	0.016
Phkg2	1.9	0.004
Pias2	-1.8	0.040
Picalm	-2.1	0.030
Pid1	-3.4	0.013
Pigl	6.8	0.002
Pigm	-6.7	0.016
Pign	-10.2	0.023
Pigp	2.8	0.000
Pih1d2	3.2	0.019
Pik3c2a	2.9	0.008
Pik3c2g	33.6	0.042
Pik3cb	27.4	0.011
Pik3r1	4.1	0.006
Pim3	2.5	0.000
Pirt	-175.4	0.015
Pkd1	2.0	0.015
Pkdcc	-2.0	0.006
Pkig	1.7	0.014
Pknox2	-19.6	0.023
Pla2g12a	2.6	0.027
Pla2g5	7.9	0.000

Pla2g7	4.0	0.046
Plag1	198.1	0.009
Plcb2	115.8	0.001
Plcg1	1.8	0.037
Plec	1.8	0.017
Plekha3	-1.5	0.036
Plekha4	6.0	0.034
Plekha8	2.4	0.045
Plekhf1	1.9	0.006
Plekhn1	867.1	0.001
Plet1	549.9	0.017
Plg	411.9	0.006
Plin1	80.0	0.021
Plod3	1.6	0.042
Pnisr	2.3	0.003
Pnpla7	4.0	0.000
Pof1b	216.9	0.003
Pold4	1.6	0.026
Poli	21.1	0.020
Polr1a,Rpa1	#N/A	#N/A
Polr2k	2.5	0.004
Polr2m	-1.9	0.015
Polr3e	-2.6	0.002
Pon2	-2.0	0.005
Pop5	2.3	0.001
Popdc3	-332.3	0.012
Porcn	1.9	0.024
Pot1	-2.8	0.013
Pou2af1	-21.5	0.030
Pou3f3	39.6	0.035
Ppa2	-2.0	0.004
Ppef2	54.9	0.024
Ppfia3	-63.7	0.003
Ppfibp2	2.3	0.002
Ppm1a	-1.7	0.013
Ppm1g	-1.6	0.007
Ppp1r10	1.5	0.040
Ppp1r14b	1.6	0.032
Ppp1r7	-1.7	0.034
Ppp1r8	2.2	0.013
Ppp1r9a	52.8	0.044
Ppp2ca	-1.6	0.039
Ppp2r1b	-2.6	0.024
Ppp2r5c	-1.7	0.011
Ppp3cc	-2.4	0.003
Ppp3r1	-2.3	0.002

Prdm2	2.4	0.048
Prdx3	-1.6	0.015
Prickle2	-2.3	0.032
Prkar1a	-1.8	0.002
Prkcd	-2.4	0.001
Prkcq	-26.1	0.034
Prkcsh	1.6	0.003
Prkx	-3.5	0.007
Prmt3	-3.0	0.003
Proc	124.7	0.029
Prokr2	-167.6	0.000
Prox2	94.0	0.031
Prpf18	2.0	0.017
Prpf38b	1.6	0.033
Prpf40a	-1.5	0.005
Prpf40b	2.0	0.042
Prps1	-2.2	0.006
Prr13	1.8	0.005
Prss12	-5.3	0.000
Prss30	-129.5	0.037
Prss8	301.4	0.003
Psat1	-4.1	0.017
Psmb10	1.7	0.028
Psmd3	-1.6	0.016
Pstpip1	4.7	0.010
Pstpip2	-18.3	0.025
Ptbp2	-4.3	0.024
Ptch2	29.1	0.050
Ptdss1	-1.9	0.001
Ptdss2	-2.0	0.003
Ptger2	113.7	0.012
Ptges	-2.5	0.006
Ptges3l1	-12.4	0.008
Ptgis	4.1	0.000
Ptgs1	-3.8	0.008
Ptgs2	-225.2	0.012
Ptk2	-1.6	0.009
Ptk7	-1.5	0.046
Ptp4a1	-2.9	0.023
Ptpn12	2.1	0.018
Ptpn2	-1.8	0.027
Ptpre	3.2	0.004
Ptprn	183.4	0.013
Ptprz1	2.3	0.017
Purb	1.5	0.046
Pvalb	33.6	0.042

Pwp2	-2.8	0.029
Pycr2	1.6	0.004
Pycrl	-1.6	0.034
Qdpr	-1.7	0.039
Rab18	-1.6	0.024
Rab1b	-2.3	0.027
Rab31	1.6	0.033
Rab39a	63.9	0.021
Rab3b	123.6	0.023
Rab5a	-3.0	0.022
Rab6b	-5.4	0.045
Rab8a	-1.6	0.000
Rabgap1l	3.5	0.037
Rabggta	-2.0	0.029
Rabggtb	1.8	0.048
Racgap1	-6.0	0.004
Rag1	-28.2	0.044
Rag2	-559.7	0.006
Ralbp1	1.8	0.026
Raly	-1.6	0.002
Ramp1	2.3	0.000
Rap1b	-2.0	0.031
Rapgef6	-3.3	0.025
Rarb	-6.7	0.006
Rasal1	681.4	0.002
Raver1	-1.8	0.008
Rbbp7	-1.9	0.002
Rbbp9	-2.4	0.023
Rbp2	106.2	0.035
Rbp2	106.2	0.035
Rbsn	-2.1	0.036
Rcbtb1	-2.9	0.020
Rcl1	-2.0	0.038
Rcl1,Clns1a	#N/A	#N/A
Rcor1	1.7	0.011
Rdh12	227.6	0.003
Rdm1	1.9	0.042
Reep2	46.7	0.012
Reep4	2.0	0.025
Reep5	1.5	0.006
Reln	-14.2	0.048
Rem2	33.0	0.040
Rev1	-2.0	0.012
Rfwd2	-1.8	0.001
Rfx6	39.6	0.039
RGD1309730	1.8	0.023

RGD1311892	64.8	0.030
RGD1560436	-96.7	0.031
RGD1561102	-168.7	0.025
RGD1564379	-1.6	0.009
Rgs10	2.0	0.009
Rgs18	-43.7	0.000
Rgs2	-2.5	0.010
Rgs3	2.0	0.003
Rgs7	-146.2	0.041
Rhd	-19.7	0.005
Rhoh	-7.6	0.025
Rhot2	2.7	0.006
Rims2	-197.4	0.003
Ring1	1.6	0.022
Riok2	-1.9	0.039
Rita1	2.6	0.003
Rnaseh1	2.0	0.040
Rnaseh2a	2.2	0.002
Rnaseh2b	-2.0	0.010
Rnf111	1.8	0.040
Rnf114	-1.6	0.002
Rnf11l1	-2.7	0.006
Rnf123	-2.1	0.009
Rnf13	-3.1	0.049
Rnf2	-2.0	0.002
Rnf215	1.7	0.041
Rnf39	148.1	0.010
Rnf4	-5.5	0.000
Rnmt	-1.9	0.009
Robo1	-4.2	0.023
Rogdi	-1.7	0.047
Rpa1	-7.4	0.002
Rpa1	-7.4	0.002
Rpain	2.1	0.014
Rpf2	-1.8	0.049
Rpgrip1l	3.4	0.023
Rpl37a	-16.5	0.043
Rpn1	-1.5	0.001
Rpp21	1.8	0.005
Rpp25	-64.6	0.001
Rps17	2.7	0.010
Rps6ka3	-3.8	0.000
Rps6kb1	-1.7	0.046
Rragc	-1.7	0.009
Rras	1.6	0.025
Rreb1	2.3	0.045

Rrn3	-3.0	0.046
Rrp8	-3.7	0.010
Rsad2	-13.6	0.007
Rsl24d1	-2.0	0.009
Rtkn2	-33.4	0.046
Rtn4rl1	3.1	0.011
Runx1	-3.3	0.012
Ruvbl2	-1.7	0.023
S100a10	2.4	0.005
S100a16	1.9	0.006
S100a3	2.3	0.044
S100a4	4.3	0.007
S100a6	4.5	0.002
Sag	36.1	0.026
Sag	36.1	0.026
Sag	36.1	0.026
Sat1	1.7	0.008
Sat1	1.7	0.008
Sat1	1.7	0.008
Saxo2	331.9	0.017
Sbds	1.7	0.016
Sbf1	1.8	0.034
Sbsn	13.7	0.002
Scap	1.8	0.028
Scara5	11.9	0.001
Scd2	-2.1	0.008
Scfd1	-1.8	0.002
Scg5	331.0	0.004
Scgb1a1	383.4	0.005
Scn2b	-11.1	0.039
Scube3	-33.8	0.023
Sdcbp	-1.5	0.026
Sdcbp2	-144.5	0.041
Sdha	-2.0	0.002
Sdr16c5	259.0	0.013
Sec13	-1.7	0.002
Sec14l1	3.1	0.000
Sec22b	-2.3	0.000
Sec23ip	-2.1	0.003
Sec24a	-3.9	0.017
Sec61a2	-2.3	0.002
Selk	1.8	0.004
Selt	-1.6	0.002
Sema3e	37.2	0.032
Sema4b	-3.0	0.004
Serp1	-2.0	0.000

Serpinb10	18.3	0.037
Serpinb2	549.6	0.001
Serpinb8	331.2	0.000
Serpinb9	-2.3	0.022
Serpine1	7.0	0.001
Serpine2	-2.1	0.022
Sesn1	-2.3	0.011
Set	-1.8	0.009
Sf3a2	-1.9	0.017
Sf3b4	-1.6	0.037
Sfi1	2.2	0.026
Sfmbt2	-147.8	0.038
Sftpc	117.9	0.019
Sfxn1	-4.0	0.003
Sfxn3	1.5	0.012
Sgcd	-2.0	0.036
Sgpl1	-6.0	0.010
Sh2d2a	-375.9	0.009
Sh3glb2	2.2	0.001
Shc4	92.0	0.022
Shmt1	-7.7	0.007
Shpk	561.9	0.000
Shtn1	14.8	0.005
Siglec10	-20.9	0.010
Sirt3	4.8	0.000
Sirt4	2.8	0.038
Sit1	-11.4	0.033
Sit1,Slc6a20	#N/A	#N/A
Skp2	-2.3	0.033
Slamf7	-169.8	0.005
Slbp	-1.6	0.042
Slc12a4	1.7	0.020
Slc13a5	3.6	0.029
Slc15a2	78.1	0.010
Slc15a3	2.6	0.020
Slc16a1	-6.2	0.001
Slc16a13	3.9	0.036
Slc16a14	45.4	0.036
Slc16a2	-5.1	0.026
Slc1a1	167.2	0.007
Slc1a2	244.6	0.008
Slc1a3	-5.5	0.000
Slc1a6	-35.1	0.014
Slc24a4	-21.9	0.032
Slc25a23	44.0	0.019
Slc25a25	-2.9	0.008

Slc25a28	1.9	0.002
Slc25a46	-1.8	0.013
Slc26a6	4.1	0.013
Slc28a1	259.0	0.018
Slc28a3	124.1	0.009
Slc30a10	-41.1	0.038
Slc30a3	-279.3	0.012
Slc30a6	-2.3	0.014
Slc30a7	-2.0	0.021
Slc35e4	2.3	0.008
Slc39a1	3.1	0.021
Slc39a14	2.0	0.048
Slc39a3	2.7	0.000
Slc39a8	-2.4	0.008
Slc43a2	3.4	0.006
Slc4a9	320.0	0.005
Slc52a3	45.5	0.029
Slc5a5	-307.9	0.015
Slc5a9	248.0	0.027
Slc6a8	2.6	0.007
Slc7a10	-229.0	0.018
Slc7a3	60.1	0.042
Slc8b1	3.2	0.002
Slc9a3	83.1	0.011
Slc9a8	-5.8	0.011
Slc9a9	-2.7	0.025
Slco4a1	16.9	0.037
Slit3	2.5	0.002
Slmo2	-1.8	0.001
Slx1b	2.3	0.001
Smad2	-2.1	0.009
Smad6	1.9	0.044
Smad7	2.6	0.012
Smagp	2.1	0.033
Smarcc1	-2.3	0.004
Smarcd1	-1.6	0.034
Smpd2	1.9	0.028
Snai2	-2.4	0.006
Snai3	192.9	0.009
Snca	-7.8	0.031
Snn	-2.3	0.047
Snrpd2	1.6	0.042
Snta1	2.0	0.005
Sntb1	83.1	0.018
Sntg2	-216.3	0.019
Snx6	-1.7	0.000

Snx9	-2.1	0.021
Soat1	-11.8	0.000
Sox12	-2.0	0.050
Sp9	-6.4	0.018
Spib	-22.8	0.001
Spn	9.9	0.002
Spn	9.9	0.002
Spp1	7.7	0.002
Spp1	7.7	0.002
Spred3	86.8	0.011
Sprr1a	2654.6	0.001
Spry1	2.1	0.029
Spsb1	-4.0	0.018
Spsb4	-59.9	0.007
Spta1	-7.7	0.043
Sptbn1	1.8	0.027
Srd5a1	-14.7	0.006
Srebf2	1.8	0.000
Srf	2.6	0.005
Srp14	1.6	0.002
Srpk3	-104.9	0.001
Srprb	-1.6	0.044
Srrm2	1.9	0.023
Srsf1	-1.5	0.023
Srsf11	1.8	0.005
Srsf4	-1.7	0.045
Srsf5	-2.3	0.000
Sspo	171.3	0.015
Sstr2	71.9	0.028
St14	2.7	0.033
St3gal2	1.9	0.004
St6galnac2	-2.5	0.001
St8sia2	-438.7	0.005
Stac2	-289.1	0.012
Stambp	-2.3	0.010
Stard7	-3.4	0.013
Steap3	1.9	0.032
Stip1	-1.7	0.049
Stip1	-1.7	0.049
Stk26	-17.3	0.009
Stk35	-3.6	0.014
Stmn2	69.6	0.043
Strada	-2.0	0.034
Stt3b	-3.0	0.003
Stx6	-1.7	0.047
Stx7	-2.5	0.011

Sulf1	3.6	0.001
Sult1a1	2.7	0.047
Sult2b1	119.1	0.023
Sumf2	-1.8	0.038
Sumo1	-1.6	0.000
Sumo2	-1.7	0.014
Suv420h1	2.0	0.014
Sv2b	69.2	0.005
Svil	2.4	0.005
Swt1	2.1	0.019
Sympk	-1.9	0.033
Syn3	-170.5	0.023
Syndig1	12.4	0.044
Syne3	58.2	0.001
Synm	4.3	0.011
Syt1	101.3	0.020
Syt17	36.4	0.040
Syt4	-47.4	0.042
Syt6	-100.7	0.028
Syt8	189.1	0.019
Syvn1	-1.5	0.033
Tacc1	1.6	0.014
Tacr1	250.9	0.011
Tacstd2	475.5	0.007
Taf1a	-4.5	0.016
Taf9b	-1.9	0.038
Tars	-2.2	0.020
Tas1r1	-96.2	0.027
Tatdn2	1.7	0.029
Tbc1d10a	1.7	0.024
Tbc1d10b	-1.7	0.026
Tbc1d20	-2.5	0.004
Tbp	-2.3	0.006
Tbx15	-75.4	0.045
Tbxa2r	-3.4	0.004
Tcf12	-2.3	0.007
Tcirg1	2.1	0.015
Tcp1	-2.3	0.007
Tdh	149.3	0.015
Tdp2	2.1	0.007
Tefm	-6.9	0.000
Tenm2	-36.6	0.049
Tep1	2.8	0.004
Tesk1	1.8	0.008
Tesk2	-6.4	0.030
Tf	-5.4	0.010

Tf	-5.4	0.010
Tfap2e	93.3	0.038
Tfb1m	1.9	0.045
Tgif2	-3.6	0.048
Thbs4	4.4	0.001
Thoc3	-1.6	0.022
Thoc5	-2.1	0.008
Thrap3	-1.8	0.025
Thsd7b	-50.1	0.016
Tiam1	45.1	0.000
Tifa	-7.3	0.000
Timd2	127.6	0.002
Timm13	1.8	0.011
Timm8b	1.6	0.043
Tiprl	-2.1	0.003
Tjp1	1.9	0.045
Tkfc	-2.6	0.028
Tle1	-2.8	0.005
Tle4	-2.2	0.016
Tlr2	-4.3	0.033
Tlr4	248.7	0.000
Tmed2	-1.8	0.002
Tmeff1	-3.0	0.004
Tmem109	1.6	0.010
Tmem135	-2.7	0.042
Tmem170b	365.8	0.003
Tmem178a	-15.2	0.010
Tmem208	1.7	0.017
Tmem259	2.0	0.009
Tmem33	2.0	0.021
Tmem43	-1.8	0.004
Tmem71	-23.7	0.034
Tmem80	2.1	0.039
Tmem86b	-12.1	0.021
Tmem9	-1.9	0.001
Tmod4	22.6	0.032
Tmprss11d	394.4	0.009
Tmprss3	-99.9	0.014
Tmprss6	-94.3	0.029
Tmprss9	12.5	0.040
Tmsb4x	2.0	0.002
Tmtc2	-4.1	0.017
Tmx1	-1.9	0.044
Tnfaip1	-2.3	0.001
Tnfrsf13b	-52.3	0.024
Tnfrsf14	18.2	0.018

Tnfrsf18	-240.7	0.012
Tnfrsf19	-3.0	0.001
Tnfsf13b	-98.6	0.029
Tnmd	-5.4	0.003
Tnnc1	-38.0	0.003
Tnnc2	964.7	0.002
Tnni1	45.5	0.038
Tnrc18	2.2	0.015
Tnrc6b	2.2	0.006
Tns3	1.8	0.030
Tob1	2.5	0.014
Tom1l1	-3.4	0.008
Tox	12.5	0.045
Tox4	-2.0	0.002
Tp53i13	1.6	0.009
Tp53inp2	1.7	0.031
Tpm1	-2.2	0.000
Tpm4	-2.2	0.001
Tpp1	1.8	0.037
Tpp1	1.8	0.037
Tppp3	3.5	0.018
Tpra1	1.6	0.012
Tra2b	-1.5	0.010
Trappc1	-1.5	0.003
Trappc4	1.9	0.002
Trex1	2.3	0.002
Trib2	2.4	0.002
Trim13	-17.1	0.020
Trim21	-46.9	0.012
Trim37	-2.7	0.038
Trim47	2.3	0.002
Trim54	187.0	0.013
Trim59	-2.1	0.040
Trim69	217.0	0.014
Trim8	1.5	0.022
Trip6	2.0	0.003
Trmt10b	2.0	0.030
Trmt10c	-1.6	0.036
Trpm1	105.4	0.018
Trpm8	-100.5	0.019
Trpv6	116.7	0.013
Trub1	-6.7	0.010
Tsacc	99.9	0.018
Tspan17	1.9	0.048
Tspan6	-1.8	0.002
Tspo	2.4	0.001

Tspyl1	-1.5	0.014
Ttbk2	4.0	0.027
Ttc12	75.4	0.013
Ttc17	2.6	0.033
Ttf2	2.0	0.031
Ttll10	112.0	0.025
Ttll3	11.4	0.043
Ttyh3	-1.7	0.012
Tuba8	199.0	0.000
Tubb2a	1.9	0.011
Tubb2a	1.9	0.011
Tubb4a	222.6	0.014
Tubgcp3	2.8	0.006
Tusc2	1.6	0.003
Txlna	-1.9	0.020
Txndc5	-1.5	0.021
Tyms	-2.2	0.025
Tyrobp	2.3	0.035
Uba1	-1.5	0.032
Uba2	-3.0	0.020
Ubac2	-2.0	0.000
Ubash3a	-67.6	0.025
Ubc	1.7	0.002
Ubd	-72.8	0.047
Ube2v2	-1.8	0.003
Ubxn2b	-7.3	0.011
Ubxn6	1.6	0.004
Uchl1	-3.3	0.001
Ucp3	494.6	0.008
Ugcg	-2.5	0.011
Ugdh	-1.8	0.015
Uhrf1	-7.7	0.015
Umps	-1.8	0.003
Unc45a	2.3	0.000
Unc5a	770.6	0.007
Unc5c	3.7	0.010
Unc5d	-35.1	0.046
Uqcc1	-1.8	0.039
Uqcr11	1.8	0.005
Uqcrq	1.6	0.034
Urb1	3.3	0.033
Use1	2.0	0.003
Use1,Ube2z	#N/A	#N/A
Usmg5	2.0	0.028
Usp11	-3.7	0.000
Usp14	-1.5	0.026

Usp19	1.8	0.041
Usp24	2.6	0.019
Usp33	2.5	0.024
Usp36	2.2	0.030
Vac14	-2.1	0.009
Vamp5	2.2	0.015
Vamp8	2.0	0.000
Vapb	-2.0	0.006
Vil1	-119.4	0.031
Vim	1.9	0.005
Vipas39	2.2	0.006
Vmac	-3.0	0.032
Vps13a	4.7	0.008
Vps13d	3.3	0.002
Vps26a	-2.1	0.021
Vps35	-1.7	0.014
Vps37b	-2.1	0.013
Vps41	-2.4	0.000
Vps52	-1.8	0.048
Vps53	1.9	0.033
Vrk2	-3.5	0.012
Vti1a	-4.4	0.001
Wars2	-5.0	0.047
Wasf2	1.6	0.028
Wasl	1.6	0.041
Wdfy3	2.8	0.009
Wdr5	-1.7	0.035
Wdr6	-1.8	0.046
Wdr75	-2.9	0.000
Wisp2	7.6	0.020
Wls	-1.6	0.034
Wnt11	-3.2	0.009
Wnt5b	2.6	0.004
Wrap73	1.7	0.042
Xk	-35.6	0.018
Xkr4	33.9	0.034
Xkr6	32.9	0.034
Xpo1	-2.2	0.025
Xpo6	-2.2	0.008
Xpot	-2.2	0.012
Xrcc1	1.8	0.002
Xrcc5	-2.6	0.001
Yaf2	-1.6	0.015
Ykt6	-2.6	0.006
Ylpm1	1.8	0.045
Ythdc1	2.0	0.025

Ywhab	-1.5	0.002
Ywhae	-1.7	0.000
Ywhag	1.7	0.014
Ywhaz	-1.7	0.004
Zbed3	-1.7	0.036
Zbp1	-40.1	0.026
Zbp1	-40.1	0.026
Zbtb16	337.2	0.001
Zbtb7c	3.5	0.018
Zc3h10	2.6	0.002
Zc3h14	-1.9	0.010
Zcchc12	-3.4	0.008
Zcrb1	1.5	0.025
Zdhhc20	-2.4	0.001
Zdhhc6	-1.9	0.012
Zfp2	247.2	0.005
Zfp263	-2.3	0.019
Zfp280b	9.6	0.029
Zfp394	2.1	0.045
Zfp410	-1.7	0.030
Zfp422	-1.9	0.003
Zfp467	2.3	0.031
Zfp483	-181.1	0.023
Zfp513	1.8	0.041
Zfp521	-2.2	0.018
Zfp641	27.7	0.033
Zfp68	-2.0	0.012
Zgpat	2.4	0.027
Zim1	-290.1	0.014
Zmpste24	-5.5	0.000
Znhit1	1.9	0.012
Znrd1	1.7	0.037
Zpbp	-114.6	0.006
Zswim5	184.5	0.008

Appendix Table 2

The original proteomic analysis data of stretched PDL cells showed in Figure 4.

Accession	Gene	LFQ intensity Control	LFQ intensity Stretched
A0A024R442	DNPEP	0	20.9996891
A0A075B785	RELCH	0	19.76844597
A0A087WTA8	COL1A2	25.22523308	26.31858635
A0A087WVZ9	POLR2E	0	20.16643715
A0A087WX58	HDGFL2	0	19.65448952
A0A087WXC5	NDUFA10	22.09055138	0
A0A087WYV8	FBN2	19.73524284	20.74386215
A0A0A0MRE1	EXOC7	0	20.59914207
A0A0A0MSK4	GPSM1	21.75103188	20.19568443
A0A0A0MTN9	FDXR	0	20.98454094
A0A0A0MTR7	RNF213	23.30827522	24.40379715
A0A0A6YYA0	TMED7-TICAM2	21.09119797	22.54521751
A0A0B4J2A0	None	0	19.78540421
A0A0C4DFM1	TM9SF4	21.73148537	20.58682823
A0A0C4DG40	SYNE1	23.24419022	24.31257439
A0A0G2JNZ5	GBA	0	22.26023293
A0A0U1RR22	PACSIN2	0	22.15375519
A0A1B0GTU1	ZC3H11B	0	17.82059097
A0A1B0GWF2	STXBP1	20.82973862	22.27295685
A0A1W2PR68	ME2	0	19.77781677
A0A2R8Y430	GSS	0	22.14416885
A0A2R8YF43	CSNK2A1	22.16628456	21.01202202
A0A3B3IS01	DARS2	19.57568359	0
B1ALD9	POSTN	21.65460205	20.32410622
B1ANM7	FAF1	21.37023354	20.30463219
B4E1E4	EIF4E2	0	19.40582275
B8ZZC5	GLS	20.10686874	0
C9JBI3	PSPH	0	18.98061371
C9JJ54	WDFY1	19.68905258	0
E7EWK3	DHX36	0	20.04686737
E9PB90	HK2	22.67480278	21.65110207
E9PF19	TBL2	21.46188927	20.36474228
E9PGM1	EIF4G1	26.33698273	24.98767471
E9PHV5	ITPRID2	19.72468948	20.93531418
E9PKU7	GANAB	0	20.05959702
E9PLK3	NPEPPS	24.54639626	25.80466843
E9PNU4	STX5	0	20.20741081
E9PQP3	ARFGAP2	0	19.8045311
F2Z2X4	XPO4	0	19.36851883
F5H4B6	ALDH16A1	20.39947319	0

F5H5N1	**NDUFS7**	0	20.1316967
F8VSC5	**SCYL2**	0	20.32432556
F8W020	**NAP1L1**	23.19088554	24.30340576
F8W1F5	**FMNL3**	0	19.6111908
F8W808	**NAA10**	21.89081955	20.4582386
F8W9T3	**SNX4**	0	21.89969635
G3V126	**ATP6V1H**	0	18.98281479
G3V529	**DDX24**	0	18.44596863
G5E9S8	**KLC1**	23.14177132	24.31741333
H0YDP7	**MRPL49**	0	20.50581551
J3KTF8	**ARHGDIA**	24.56307983	25.60501099
J3QLR8	**MRPS23**	0	19.49917221
J3QR09	**RPL19**	22.55912781	23.77283669
M0R026	**ILVBL**	21.18252945	19.68642235
M0R208	**CLPP**	20.40789795	22.10980606
O00267	**SUPT5H**	0	20.00237083
O00754	**MAN2B1**	0	20.7157383
O14818	**PSMA7**	24.01154327	25.14390373
O15173	**PGRMC2**	22.74915123	23.92315865
O15270	**SPTLC2**	0	19.53425407
O15427	**SLC16A3**	23.23410606	22.17292023
O15460	**P4HA2**	24.34638023	26.01073265
O43390	**HNRNPR**	21.59418488	23.08321571
O60502	**OGA**	0	21.01352119
O60762	**DPM1**	19.60188293	20.8239994
O75534	**CSDE1**	21.91338539	22.95976639
O75643	**SNRNP200**	26.44395256	25.00906754
O75844	**ZMPSTE24**	21.97571754	20.68953133
O75962	**TRIO**	20.65394783	21.80644417
O75976	**CPD**	0	21.04092979
O94804	**STK10**	0	17.59433937
O95197	**RTN3**	22.27332687	20.819561
O95248	**SBF1**	0	21.51123238
O95810	**CAVIN2**	0	19.57767677
O95881	**TXNDC12**	0	20.94177628
O96005	**CLPTM1**	22.37983513	21.17718506
P02452	**COL1A1**	26.02312088	28.7821312
P02461	**COL3A1**	21.85866928	23.9216156
P02545	**LMNA**	28.88495064	29.89865112
P02792	**FTL**	23.62644958	22.54158401
P04080	**CSTB**	23.54957199	22.35901451
P04632	**CAPNS1**	24.03204155	25.27476311
P04792	**HSPB1**	26.62714577	27.82420158
P04818	**TYMS**	21.41142082	20.24898911
P05997	**COL5A2**	19.73646545	21.18924332
P07814	**EPRS**	24.96146393	26.25281143
P08243	**ASNS**	22.13842964	23.32909775

P08574	**CYC1**	0	20.90873909
P08648	**ITGA5**	25.22574806	24.18737221
P09960	**LTA4H**	21.50149727	22.81188202
P0DMV9	**HSPA1B**	29.0905323	27.32551575
P12081	**HARS**	24.30528641	25.34235001
P14923	**JUP**	20.95695114	0
P15104	**GLUL**	0	20.75287056
P16234	**PDGFRA**	0	20.9249897
P16930	**FAH**	21.85178566	20.74779892
P17066	**HSPA6**	28.77596092	27.75748062
P19174	**PLCG1**	0	19.5958519
P19474	**TRIM21**	0	19.35287476
P20908	**COL5A1**	21.16090965	22.27810097
P21964	**COMT**	22.38226509	23.46811867
P23381	**WARS**	23.40743256	24.44335365
P24928	**POLR2A**	20.53763199	19.08085442
P26022	**PTX3**	0	19.87612724
P26038	**MSN**	28.74890327	29.82072258
P26373	**RPL13**	25.4160614	26.60385323
P27348	**YWHAQ**	26.22118187	27.4228611
P28288	**ABCD3**	21.29283142	19.83644104
P30038	**ALDH4A1**	0	18.69149208
P30405	**PPIF**	23.03175545	22.02116776
P31153	**MAT2A**	23.43478966	22.30924797
P32119	**PRDX2**	25.56575584	24.35137749
P32455	**GBP1**	20.91342163	22.04620171
P35354	**PTGS2**	22.50054932	20.74246407
P35573	**AGL**	0	18.90124321
P42167	**TMPO**	20.45352364	21.76198578
P43487	**RANBP1**	22.69242859	23.94628143
P46821	**MAP1B**	27.4512043	26.03632545
P46937	**YAP1**	21.46173859	22.57327652
P46940	**IQGAP1**	27.27382088	28.48834229
P47914	**RPL29**	23.20067596	24.29459953
P49748	**ACADVL**	25.07842827	26.20894051
P50395	**GDI2**	26.025383	27.03128433
P50416	**CPT1A**	23.39610672	22.20943451
P51809	**VAMP7**	0	19.97687149
P51970	**NDUFA8**	21.54297638	19.81770515
P52630	**STAT2**	20.81151009	21.92524338
P55084	**HADHB**	25.01979446	23.79213333
P56545	**CTBP2**	21.70956612	22.81381989
P57764	**GSDMD**	0	19.04390907
P61586	**RHOA**	0	22.79070282
P61619	**SEC61A1**	24.79808044	23.63533401
P62826	**RAN**	25.3025341	26.37102509
P67809	**YBX1**	25.56435966	24.45349884

P78559	**MAP1A**	23.87107658	24.99183273
Q00688	**FKBP3**	21.51638603	23.73106956
Q04917	**YWHAH**	24.16622353	25.20988846
Q06124	**PTPN11**	21.06716919	22.37581062
Q06203	**PPAT**	0	20.50057411
Q08378	**GOLGA3**	21.67620277	22.77782059
Q12965	**MYO1E**	20.13746071	21.31959343
Q13131	**PRKAA1**	0	21.00422287
Q13242	**SRSF9**	19.10469627	20.44909668
Q13596	**SNX1**	21.8387661	23.32991982
Q14152	**EIF3A**	24.92718887	26.21811676
Q14696	**MESD**	19.84509277	21.00374222
Q14789	**GOLGB1**	24.66871452	23.57080078
Q15021	**NCAPD2**	0	20.3668766
Q15056	**EIF4H**	23.36826324	24.77660751
Q15075	**EEA1**	23.31741333	24.69104385
Q15233	**NONO**	24.7138195	25.76789665
Q16134	**ETFDH**	21.16029549	0
Q16513	**PKN2**	19.69333076	20.82150841
Q16658	**FSCN1**	25.69144249	26.86714554
Q16778	**HIST2H2BE**	26.90644264	25.62419128
Q16822	**PCK2**	22.51982117	24.02647972
Q16878	**CDO1**	0	23.31451225
Q5JRG1	**NUP58**	0	20.33123207
Q5T0I0	**GSN**	21.1754818	22.3467598
Q5VYK3	**ECPAS**	22.48892975	24.10093307
Q68CQ7	**GLT8D1**	0	21.56592941
Q68E01	**INTS3**	0	19.13560867
Q6P2E9	**EDC4**	19.89511681	21.12760925
Q7Z3U7	**MON2**	0	21.72558975
Q8IVF2	**AHNAK2**	21.0956459	0
Q8IWJ2	**GCC2**	20.04126358	21.07463455
Q8N129	**CNPY4**	19.50589371	0
Q8TBA6	**GOLGA5**	19.2819519	0
Q8TCT9	**HM13**	25.04963684	24.03355408
Q8TDD1	**DDX54**	0	19.40621758
Q8TEX9	**IPO4**	21.96370506	23.04977798
Q8WU90	**ZC3H15**	20.30273628	21.33576393
Q92575	**UBXN4**	0	20.73073959
Q92629	**SGCD**	0	19.04788017
Q92734	**TFG**	23.73055267	24.79872322
Q92882	**OSTF1**	20.70497513	21.89145088
Q96CG8	**CTHRC1**	21.28263092	22.5556221
Q96CT7	**CCDC124**	0	19.65881729
Q96JQ0	**DCHS1**	18.9074192	0
Q96SB3	**PPP1R9B**	21.21299934	0
Q96TA1	**FAM129B**	26.7624321	24.93035126

Q99715	**COL12A1**	25.5644474	27.04228592
Q99747	**NAPG**	0	20.63962364
Q99805	**TM9SF2**	21.15961838	20.02431679
Q99832	**CCT7**	25.16970634	26.43934822
Q9BPW8	**NIPSNAP1**	0	20.66440201
Q9BQ67	**GRWD1**	0	19.73229599
Q9BQS8	**FYCO1**	20.9930687	22.06111526
Q9BRF8	**CPPED1**	0	21.15165138
Q9BW60	**ELOVL1**	22.21208	21.1392746
Q9BY44	**EIF2A**	22.04266739	20.94713783
Q9H1B7	**IRF2BPL**	0	18.87306595
Q9H223	**EHD4**	0	20.26956558
Q9H2U2	**PPA2**	0	21.18507385
Q9HAV7	**GRPEL1**	20.83259964	22.38094521
Q9HB40	**SCPEP1**	0	20.93675232
Q9HCL0	**PCDH18**	0	19.58913612
Q9HD45	**TM9SF3**	22.06999016	20.69251251
Q9NRY4	**ARHGAP35**	0	19.44497871
Q9NSD9	**FARSB**	22.56020164	24.20329285
Q9NUQ8	**ABCF3**	0	19.8791523
Q9NV70	**EXOC1**	19.37553596	0
Q9NVI7	**ATAD3A**	22.91378593	24.31319809
Q9NW15	**ANO10**	0	20.39089584
Q9NX08	**COMMD8**	0	20.09493828
Q9NXG2	**THUMPD1**	0	21.14413834
Q9NZB2	**FAM120A**	25.2062397	23.61717224
Q9NZN4	**EHD2**	25.39447212	26.43766594
Q9P2R3	**ANKFY1**	21.45848846	22.65425301
Q9UBG0	**MRC2**	23.40781975	24.75302315
Q9UH99	**SUN2**	19.84743309	21.2696228
Q9UL25	**RAB21**	21.68863487	22.91340256
Q9ULT8	**HECTD1**	0	20.53107643
Q9UMX0	**UBQLN1**	0	21.44955063
Q9UN70	**PCDHGC3**	0	20.26647949
Q9UNW1	**MINPP1**	0	20.22163963
Q9UQE7	**SMC3**	22.4522171	21.36420822
Q9Y224	**RTRAF**	22.34708405	23.44113731
Q9Y230	**RUVBL2**	23.94529915	24.95464706
Q9Y281	**CFL2**	0	21.72425652
Q9Y2X3	**NOP58**	0	21.9932766
Q9Y3I0	**RTCB**	23.71187782	24.85562134
Q9Y512	**SAMM50**	0	21.21240616
Q9Y5S2	**CDC42BPB**	19.38237	20.63794518
Q9Y5S9	**RBM8A**	21.61867332	20.58389473
Q9Y608	**LRRFIP2**	0	20.42070007
R4GNG3	**GIT2**	0	19.97084808
S4R3Z2	**AKR1C3**	21.77671814	0

Appendix Table 3

The antibodies, primers and protein used in the study.

Primary antibodies (Immunofluorescence)					
Antigen	**Figure**	**Diluting factor**	**Company**	**Cat. No.**	**Batch No.**
Notch 1 ICD	2D	1:200	e-Bioscience	14-5785-82	E04375-261
Total Notch1	2E	1:200	Cell Signalling	4380s	lot 2
Dll1	2F	1:200	R&D Systems	AF5026	
Osteopontin	2G	1:100	Dr Larry fisher (NIH)	LF-166 hOPN (C-terminus)	
Periostin	1C, 3H-J, App. 2A	1:400	Abcam	AB14041	
Notch 2 ICD	2E	1:200	Sigma	SAB4502022	410353
Lamin A/C	5B	1:200	Cell signalling	4777s	Lot 1
Lamin A/C	5E	1:200	Santa Cruz	sc-20681	A1116

Secondary antibodies (Immunofluorescence)				
Target	**Dilution**	**Company**	**Cat. No.**	**Lot**
Alexa 568 Donkey anti-Mouse IgG	1:500	Life Technologies	A10037	1303018
Alexa 568 Donkey anti-Rabbit IgG	1:500	Life Technologies	A10042	1964370
Alexa 568 Donkey anti-Rabbit IgG	1:500	Abcam	Ab175470	
Alexa 488 Donkey anti-Sheep IgG	1:300	Life Technologies	A11015	1322311
Alexa 488 Donkey anti-Mouse IgG	1:300	Life Technologies	A21202	1796361

Antibodies (Western Blotting)					
Antigen	**Figure**	**Diluting factor**	**Company**	**Cat. No.**	**Batch No.**
GapDH	5	1:500	Santa Cruz	SC-32233	H2114
Lamin A/C	5	1:400	Cell Signalling	4777	
Anti-Rabbit HRP	5	1:500	Cell Signalling	7074P2	
Anti-Mouse HRP	5	1:500	Cell Signalling	7076P2	

Primers			
Gene (mouse)	**Forward primer ('5-'3)**	**Reverse primer ('5-'3)**	**PCR Product size**

Hes1	TGAGCCAGCTGAAAACACTG	AGCACACTTGGGTCTGTGC	160
DLL1	GCACGGACCTCAAGTACTCC	ATGCTGCTCATCACATCCAG	200
Hey1	CTTTTGGTGCATGGAACTGT	CAGTTCAGTGGAGGTCGTTT	152
DLL4	GCGAGAAGAAAGTGGACAGG	ATTCTCCAGGTCATGGCAAG	185
Jag1	ATCGTGCTGCCTTTCAGTTT	ATTGCAGCCAAAGCCATAGT	234
Acta2	CAGATGTGGATCAGCAAACA	TGGCTAGGAATGATTTGGAA	161
BGLAP	CAGCGAGGTAGTGAAGAG	GGGAAGAGGAAAGAAGGG	249
Runx2	CTCTGACCGCCTCAGTGATT	GGCTCAGGTAGGAGGGGTAA	200
Periostin	CAAAACTGAAGGACCCACAC	TATTTCCACAGGCACTCCAT	154
Sparc	GTGCAGAGGAAACCGAAGAG	AAGTGGCAGGAAGAGTCGAA	200
GapDH	ATCACTGCCACCCAGAAGAC	CAGTGAGCTTCCCGTTCAG	148
36B4	GCAATGTTGCCAGTGTCTGT	GCCTTGACCTTTTCAGCAAG	142
SPP1	TTGCAGTGATTTGCTTTTGC	GTCATGGCTTTCGTTGGACT	200
Dlk1	GGCTTCATCGACAAGACCTG	CAGGTCTCGCACTTGTTGAG	185

Recombinant Proteins			
Protein	**Company**	**Cat. No.**	**Lot**
Human Jagged 1	R&D	1277-JG-050	RZL1713041